Energy Conversion and Management 320 (2024) 119013

Contents lists available at ScienceDirect

Energy Conversion and Management

journal homepage: www.elsevier.com/locate/enconman

Development and simulated evaluation of inter-seasonal power-to-heat and power-to-cool with underground thermal storage for self-consumption of surplus solar energy in buildings

Fabian Eze [a,b], Wang-je Lee [b], Young sub An [b], Hongjin Joo [b], Kyoung-ho Lee [b,*], Julius Ogola [c], Julius Mwabora [a]

[a] Department of Physics, University of Nairobi, 30197 – 00100 Nairobi, Kenya
[b] Renewable Energy System Laboratory, Korea Institute of Energy Research, 152, Gajeong-ro, Yuseong-gu, Daejeon 34129, Republic of Korea
[c] Department of Mechanical and Manufacturing Engineering, University of Nairobi, 30197 – 00100 Nairobi, Kenya

ARTICLE INFO

Keywords:
Underground thermal storage
Air source heat pump
TRNSYS Simulation, Space heating and cooling
Inter-seasonal self-consumption
Surplus renewable energy

ABSTRACT

The adoption of renewable energy, such as solar, to meet the energy demand in buildings has become one of the keys to achieving the global target for net-zero emissions. As a result, solar photovoltaic installations have increased tremendously, giving rise to an enormous surplus of electricity generation, which has become an issue requiring alternative ways to be addressed. Underground thermal energy storage for power-to-heat operations has gained interest in this area due to its reliability, cost-effectiveness, and carbon-free nature. This study presents a novel system configuration with an operational strategy guided by a simple control method that uses surplus photovoltaic electricity to power an inter-seasonal heating and cooling system coupled with seasonal underground thermal energy storage. Two cases were developed, modeled, and simulated in the TRNSYS 18 simulation tool. Case 1 involves an air-source water-load heat pump and 1.5 m-shallow underground thermal storage with power-to-heat and power-to-cool operations. Case 2 features an air-source water-load heat pump and vertical 150 m-deep underground thermal storage with power-to-heat and power-to-cool operations. The base case involving an air-source water-load heat pump without power-to-heat and power-to-cool operations was modeled for their evaluation. In Case 1, energy savings and power-to-heat and power-to-cool efficiency of 14 % and 39 % were obtained, respectively. Similarly, energy savings and power-to-heat and power-to-cool efficiency of 13 % and 36 % were obtained, respectively, from Case 2. Both study cases displayed a self-consumption ratio of approximately 81 % compared to the base case, which had 76 %. Similarly, the surplus energy utilization ratio of about 26 % was obtained from both cases. Furthermore, 60 % and 52 % thermal efficiencies were obtained for study cases 1 and 2, respectively, for the underground thermal storage. The results demonstrate that the configuration and operational strategy implemented can seasonally utilize the available photovoltaic power and enhance the performance of the heat pumps.

1. Introduction

Deploying more energy-efficient technologies in buildings plays a key role in meeting the global energy demand and reducing greenhouse gas emissions [1]. Over the past decade, global energy consumption in buildings has increased by an average of 1 % annually. Notably, space heating and water heating together account for approximately 45 % of energy demand in buildings and are responsible for about 80 % of CO_2 emissions from the building sector [2]. However, the demands for building space and water heating must be met to satisfy human comfort. For this reason, about 60 % of heating and cooling energy demands are still met using fossil-fuel-related systems [3]. Moreover, energy from fossil fuels appears to fluctuate in price and has been forecast to deplete entirely in the foreseeable future, in addition to its massive impact on the environment [4]. This begs for relentless research into more efficient and low-carbon heating and cooling.

1.1. Background and motivation

The use of renewable energy (RE) sources such as solar energy as an alternative energy source for space heating and cooling has proven to be

* Corresponding author.
E-mail address: khlee@kier.re.kr (K.-h. Lee).

https://doi.org/10.1016/j.enconman.2024.119013
Received 15 April 2024; Received in revised form 16 August 2024; Accepted 1 September 2024
Available online 5 September 2024

Nomenclature

Symbols and Abbreviations

Symbols	Meaning
T_{in}	Inlet water temperature (°C)
T_{out}	Outlet water temperature (°C)
T_{inf}	Temperature of infiltrating air (°C)
T_z	Temperature of zone (°C)
$T_{ambient}$	The ambient temperature (°C)
$\dot{m}$	Mass flow rate (kg/hr)
c_p	Specific heat capacity (kJ/kg·K)
Q	Heat gain/loss (kW)
$\dot{Q}_{cool/heat}$	Cooling or heating rate (kW)
E_{com}	Power consumption of heat pump compressor (kW)
E_{fan}	Power consumption of heat pump fan (kW)
E_{conv}	power consumption of the conventional heat pump (kW)
E_{test}	power consumption of the test heat pump (kW)
E_{p2hc}	Power consumption of heat pump during UTES charging (kW)
UA	Product of zone loss coefficient and the zone area (kJ/hr·K)
C	The zone capacitance (kJ/K)
ρ	Density (kg/m^3)
V	Volume (m^3)
c_{ps}	Heat capacity of soil (kJ/m^3/K)
V_s	Volume of the borehole (m^3)
t	Time (hour)
Q_{Load}	Building load (kW)
$Q_{BT2load}$	Heat transfer to load from the buffer tank (the met load in kW)
$Q_{HP2water}$	Heat transfer to the liquid on the heat pump load side (kW)
E_{HP}	Power consumption of the heat pump (kW)
$Q_{UTES,c-d}$	Fluid-to-ground heat transfer from heat pump to UTES during charging in spring and autumn and during discharging in winter and summer (kW)
$E_{pv,total}$	Total PV power generation per given time (kW)
$E_{pv,P2HC}$	Total annual PV Power consumed by heat pump for P2HC operation (kW)
$E_{pv,used}$	Total PV power consumed per given time (kW)
$E_{pv,surplus}$	Surplus PV power generation per given time (kW)
$E_{pv,HnC}$	Total PV power consumed during winter heating and summer cooling (kW)
$E_{pv,etc}$	Total PV power used for other electricity demands of the building including lighting and water pumps (kW).

Subscripts

a	air
w	water
hp	Heat pump
iandf	Initial and final
candd	Charge and discharge

Abbreviations

ASHP	Air Source Heat Pump
ASWL	Air-source water-load
COP	Coefficient of Performance
DHW	Domestic Hot Water
P2HP2C	Power-to-heatPower-to-cool
PCM	Phase Change Material
PV/PVT	Photovoltaic/Photovoltaic Thermal
PVSC	Photovoltaic self-consumption
PVSS	Photovoltaic self-sufficient
SAHP	Solar-assisted heat pump
sUTES	Shallow Underground Thermal Energy Storage
TES	Thermal Energy Storage
TRNSYS	Transient System Simulation Program
UTES	Underground Thermal Energy Storage

one of the best methods of alleviating the issue of greenhouse gas emissions and the resulting climate change emanating from using fossil fuels [4]. However, their time-dependent is a big challenge and requires an efficient and reliable storage system [5]. Nowadays, many countries are proposing policies that would require commercial buildings to increase their use of renewable energy to meet a certain percentage of their electricity demand [6]. This would require the widespread adoption of solar PV self-consumption (PVSC) and PV self-sufficient (PVSS) systems. Solar PVSC system implies an installed PV system where energy generation is primarily consumed on-site rather than exported to the grid [7]. On the other hand, its self-sufficiency goes a step further from self-consumption by meeting all the energy needs of the facility without relying on the national grid or other external sources [8]. Consequently, these extensive solar installations generate a significant surplus of electricity seasonally, especially during the seasons with moderate weather conditions when heating and cooling are less required.

It is crucial to find an optimal method of utilizing this surplus energy, including its conversion to heat using thermal energy storage, which can be applied to water heating [9] and building space conditioning. In Europe, for example, some studies have discussed the issue of surplus energy existence, especially in self-consumption PV systems, and the possible ways of utilizing them. The recent study by Lienhard et al. [10] investigated the electricity situation from renewable energy (RE) sources using published data scenarios. The study proved that seasonal imbalances exist in Switzerland and its neighboring nations and asserted that this situation could affect reaching the net zero target of Switzerland and Europe as a whole. Ordóñez and Hernández [11] studied the self-consumption PV system installed on university buildings and found that it is economically viable to match the PV production and consumption. Roldán-Fernández et al. [12] studied the application of a self-consumption PV system for a domestic building adopting a ceteris paribus technique and discovered, in general, a reduction in the market-traded demand to about 2 %. In the United States, Delholm et al. [13] and Tabassum et al. [14] found that surplus electricity from renewable energy systems such as solar due to inadequate storage systems is a challenge that must be addressed. Similarly, in Australia, Yildiz et al. [15] investigated the potential of saving the surplus PV power production in a residential electric water heating technology and found that surplus PV power production from a 4.5 kW system can be utilized to provide about 48 % of domestic hot water demand of a household accounting for about 28 % self-consumption. In Korea, some studies have been carried out to ascertain the severity of the situation. For example, Liao et al. [16] quantified the existence of excess PV electricity, questioning the *when* and *where* the PV electricity redundancy occurs by examining a residential and an office buildings. The study found that surplus PV electricity exists in both buildings and has its peak during late spring and the beginning of summer. An et al. [17] analyzed PV systems installed in residential and non-residential buildings, and the study showed that the installed PV systems contribute 139.0 % of energy production in autumn, winter, and spring. Although the system achieved self-sufficiency, surplus electricity generation exists, and this occurs highly during the spring and autumn seasons. In addition, Kim et al. [6] mentioned in their quest to investigate the surplus electricity production trends that during spring and autumn, electricity demand decreases, allowing excess electricity generation from PV systems to increase significantly.

Over the years, various methods have existed for utilizing surplus PV electricity, of which the most common is integration into the national grid. However, as discussed by Shafiullah et al., [18] and Shaik et al. [19], this poses a big technical challenge by disrupting the voltage and frequency stability as well as the demand ramping rates. Also, lithium-ion batteries have been employed for use in balancing the time-mismatch of PV power generation, however this poses a challenge of none cost-effectiveness and faster degradation of life [20]. Further strategies for utilizing the excess electricity production from solar PV systems have been studied. For instance, Vaziri Rad et al. [21] reviewed the methods of using excess electricity from solar PV systems, which include power-to-gas (P2G), which is the conversion of surplus energy to gases such as methane (CH_4) [22], power-to-heat (P2H), which is the conversion of power to heat using a heat transfer medium or fluid such as water [23], power-to-hydrogen (P2Hy), which is the conversion of power to hydrogen through a process such as water electrolysis [24], among others. The study found that P2H is a low-cost method that requires further research, while P2G and/or P2Hy constitute the issues of low volumetric efficiency and storage problems. Wang et al. [25] studied the possibility of improving PVSC and PVSS systems that can provide water heating and space conditioning in a residential building. The system combined a PV system, heat pump, hot water storage vessel, and batteries. The results showed that this integration could enhance the PVSC and PVSS by 40.24 % and 86.63 %, respectively. Gravelsins et al. [26] performed research involving the installation of large solar PV for district heating and found that it is not cost-effective to install large sizes of PV for consumption in one season. However, the authors proposed a P2H technique that could utilize about 45 % of the surplus energy produced by the installed PV capacity.

A balance between generation and consumption can be provided by leveraging power-to-heat (P2H) and power-to-cool (P2C) approaches to utilize surplus PV electricity effectively [27]. However, one of the primary issues in its application includes the lack of a sophisticated system configuration with an operational strategy coupled with simple or complex control methods to accomplish this balancing [28]. A little progress has been made on this topic, and even with the few studies, more efficient, cost-effective, and durable storage systems are still required. Furthermore, an efficient operation of a self-consumption PV system for inter-seasonal surplus electricity consumption is currently in high demand. To tackle these pressing issues, incorporating underground thermal energy storage (UTES) into solar PV systems for use with heat pumps is necessary [29]. Among other thermal energy storage systems such as conventional insulated tanks (CIT), phase change materials (PCM), and vacuum insulated tanks (VIT), UTES appears to be more reliable and cost-effective depending on the type of configuration and depth [30], although its efficiency may be retarded due to thermal losses, necessitating insulation [31]. The ground beyond specific depths maintains a stable temperature, providing this method an advantage over other energy storage methods [28]. In addition, it possesses a low-cost and thermal efficiency advantage over the P2G and/or P2Hy techniques, which have disturbing issues with cost, volumetric efficiency [32], and storage [33]. They can be horizontal or vertical types, with various other sub-categories [34]. The major difference between these configurations lies in their storage capacities and depths, which are directly related to the overall installation costs [35]. The deeper the system, the higher the overall cost, even though land spaces may be saved; therefore, shallow UTES have become a better option [36]. Some studies have been carried out on shallow UTES with depths ranging from 1.5 m to 10 m [37] and also on deep UTES where the availability of land is limited or for commercial resident applications [38]. Shallow UTES can be classified primarily into closed-loop and open-loop types, where in the closed-loop type, the working fluid is forced to circulate through pipes buried in the ground, and in the open-loop type, the reverse is the case [37]. The UTES can be charged directly or indirectly using solar-assisted heat pumps (SAHP) or solar PV systems. These storage systems are particularly useful in addressing the issue of inconsistent solar energy supply by providing the necessary energy during off-peak hours or for the efficient operation of heat pumps during extreme weather conditions.

1.2. Gaps, Novelty, and Objectives of the Study

Previous literature has highlighted the global concern of the existing surplus energy from solar energy systems such as PV systems, a trend that is anticipated to persist as numerous countries aim to achieve their renewable energy penetration targets for net-zero emissions. Therefore, approaches such as power-to-heat (P2H) and power-to-cool (P2C) should be explored. The Power-to-heat and cool (P2HC) strategy is one of the reliable methods of solving this issue by balancing generation and consumption. However, its application is hindered by a lack of sophisticated system configuration with an operational strategy coupled with simple or complex control methods to accomplish this balancing. Additionally, the literature lacks a study on the inter-seasonal consumption of surplus PV energy with integrated UTES and heat pumps, leaving surplus redundant PV power, especially in spring and autumn. In most cases, daily self-consumption had been studied without inter-seasonal consideration. Furthermore, the efficient operation of dual-source heat pumps by using air and water on the source side is necessary to improve the heat pump's efficiency and result in substantial energy savings in heating and cooling applications. Still, this practice has been limited in previous studies. Therefore, to achieve optimal results with heat pumps and to allow for maximum inter-seasonal utilization of surplus energy using UTES, an integrated use of heat pumps and UTES with a corresponding operational strategy guided by simple control methods is essential.

This study presents a system configuration and operational strategy guided by simple control methods that allow for the effective and inter-seasonal utilization of excess PV power generation in buildings. This is accomplished by integrating UTES, where the operational strategy and control method allow surplus electricity to charge the UTES during seasons with little or no heating and cooling demands and extract the stored heat to assist the heat pump during seasons of high heating and cooling demand. The PV system with heat pump and UTES for P2HC operation was developed and simulated in the TRNSYS 18 simulation tool. The overall system comprises a solar PV system, different heat pump configurations, shallow and vertical UTES, and the building load. The heat pump exhibits dual functionality where air and water are applied on the source side. The proposed system simulation was applied to a public school building in Seoul, Korea, for performance evaluation considering two cases. A conventional system of air-source water-load (ASWL) heat pump without P2HC configuration was also modeled as a baseline for the performance evaluation of each case study. Although the system was evaluated under conditions reflecting the four distinct seasons, such as the South Korean climate, its configuration allows for universal use with simple modification of its control methods to represent the time of occurrence of surplus energy.

2. Methods

The intermittent nature of renewable energy has led to an in-depth exploration of various energy storage methods besides battery storage systems. These methods involve converting electricity generated by renewable energy sources such as solar energy into gas (power-to-gas) [39], heat for heating (power-to-heat), or heat for cooling (power-to-cool) during the off-peak periods [40].

2.1. Concept of inter-seasonal Power-to-Heat and cool

In this study, the inter-seasonal P2H and P2C operations extract surplus energy from solar PV systems and convert it to heat for heating and cooling purposes by using heat pumps and thermal storage. The operational strategy involves self-detection of surplus electricity and

utilization by conversion and storage to summer cooling energy in spring and winter heating energy in autumn. This operational strategy is represented in Fig. 1. During winter, the energy demand for space heating is high with a corresponding low PV electricity, similar to the summer season with high space cooling energy demand. However, the energy demand for either space cooling or heating is less during the spring and autumn seasons as a result of their moderate weather conditions. During these seasons, surplus PV electricity exists. In spring, the excess PV electricity is used for charging the TES with cold heat (P2C operation) for use during summer cooling. Similarly, in autumn, it is used for charging the TES with hot heat (P2H operation) for use during the winter heating. The charged cool and warm thermal energy in thermal storage is utilized as the heat source of the heat pump for space cooling and heating by cooling and heating source air temperature, respectively. The heat pump consumes the surplus PV energy by utilizing it for charging the thermal energy storage.

2.2. Overall system configuration

The intended building comprises solar PV installed, as shown in the energy flow diagram in Fig. 2 a). The system configuration is such that the electricity generated from the solar PV is used for the operation of the heat pumps, which are used for providing heating and cooling energy needs for the building. In general, conventional air-source air-load (ASAL) heat pumps are widely used for space heating and cooling in building applications; however, the present study explores the use of ASWL heat pumps. As shown in Fig. 2 b), during the non-heating and non-cooling (spring and autumn) periods, the P2HC strategy is employed where the UTES is charged by the heat pump. The heat pump functions as an air-source water-load during this time and uses the excess electricity from solar PV for operation. During the heating and cooling period, the heat pump also functions as an air-source water-load heat pump; however, the source air inlet to the heat pump is preheated or precooled by the charged warm and cool thermal energy from the UTES using an air–water heat exchanger (HX). In general, the heat pump functions as a dual-source (air and UTES) water-load heat pump and is solely operated by using the energy generated from solar PV, thereby meeting self-consumption requirements.

2.3. Operational method and control

Successful application of the aforementioned system configuration is dependent on the implementation of a well-designed operational strategy. The system is designed to operate in four seasons – winter, spring, autumn, and summer – throughout the year. It is assumed that the heating operations begin on November 1 at the 7296th hour and end on March 31 at the 2160th hour. After that, spring lasts from April 1st to May 31st, summer from June 1st to August 31st, and autumn from September 1st to October 31st. During the moderate weather conditions of spring and fall, there is little or no need for heating or cooling, rather, surplus energy from PV systems exists. The operational strategies of the system configuration demonstrated in Fig. 2 b) is such that, during winter heating and summer cooling operations, the controlled flow diverter (CFD) controls the flow from the UTES towards the pump, P1, which is activated. The valve, V1, is used to return the flow from the HX to the UTES for cycle completion. During P2C and P2H operations in spring and autumn, respectively, the CFD controls the flow from the UTES towards the pump, P2, which is activated. Again, the valve, V1, is used to return the flow from the HP to the UTES for cycle completion. During winter heating, warm heat stored in the UTES is used to pre-heat the ambient air, which is supplied as the HP air source. During summer cooling, cold heat stored in the UTES is used to pre-cool the ambient air, which is supplied as the HP air source. It is assumed that no heating or cooling is required during spring and autumn. In spring, P2C operation takes place, while P2H operation takes place in autumn. During these seasons, unheated/uncooled ambient air is supplied as the HP air source, with water on the load side for charging the UTES. The control method for this operation is such that the ASWL P2HC operation is only activated when excess electricity from the PV system exists in spring and autumn, and the HP outlet water temperature is within the setpoint for P2C or P2H. Only then is pump P2 activated; otherwise, it remains off. This is translated numerically as shown in equations (1) and (2). The HP outlet temperature is ensured to remain above 2°C during P2C and below 50°C during P2H operations to avoid supplying a freezing temperature to the UTES.

$$If\ P2C\,(t_{i-1}) = ON/OFF \begin{cases} P2C(t_i) = ON if E_{pv,surplus} > 0 \\ P2C(t_i) = OFF if E_{pv,surplus} < 0 \end{cases} \quad (1)$$

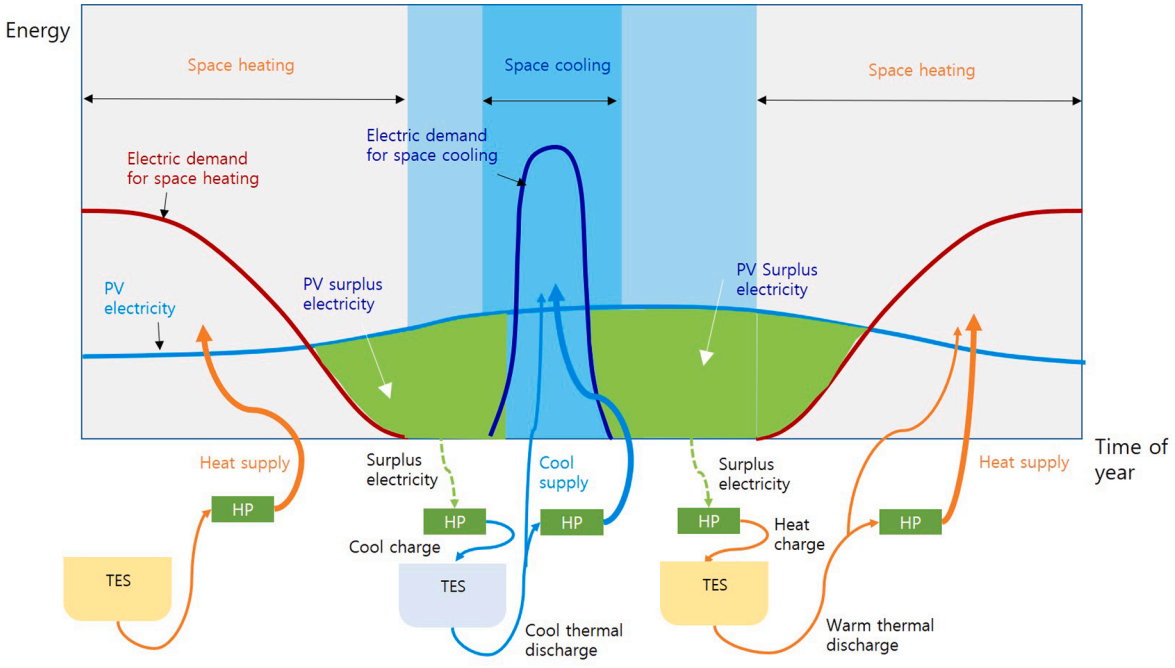

Fig. 1. The concept of the inter-seasonal P2H and P2C of the study.

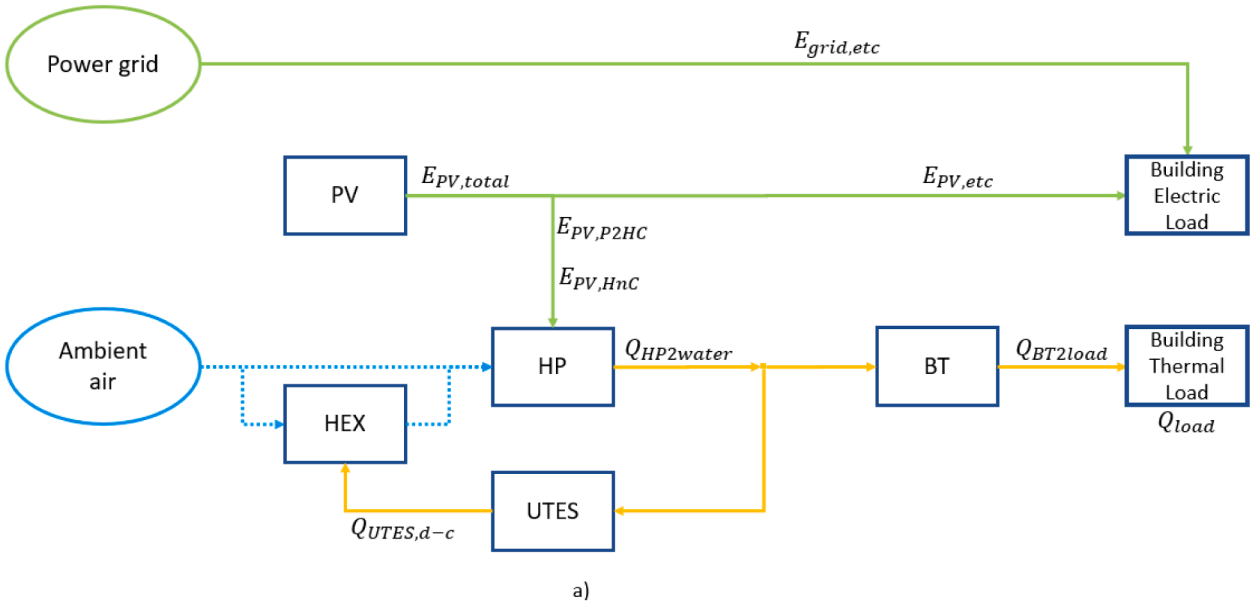

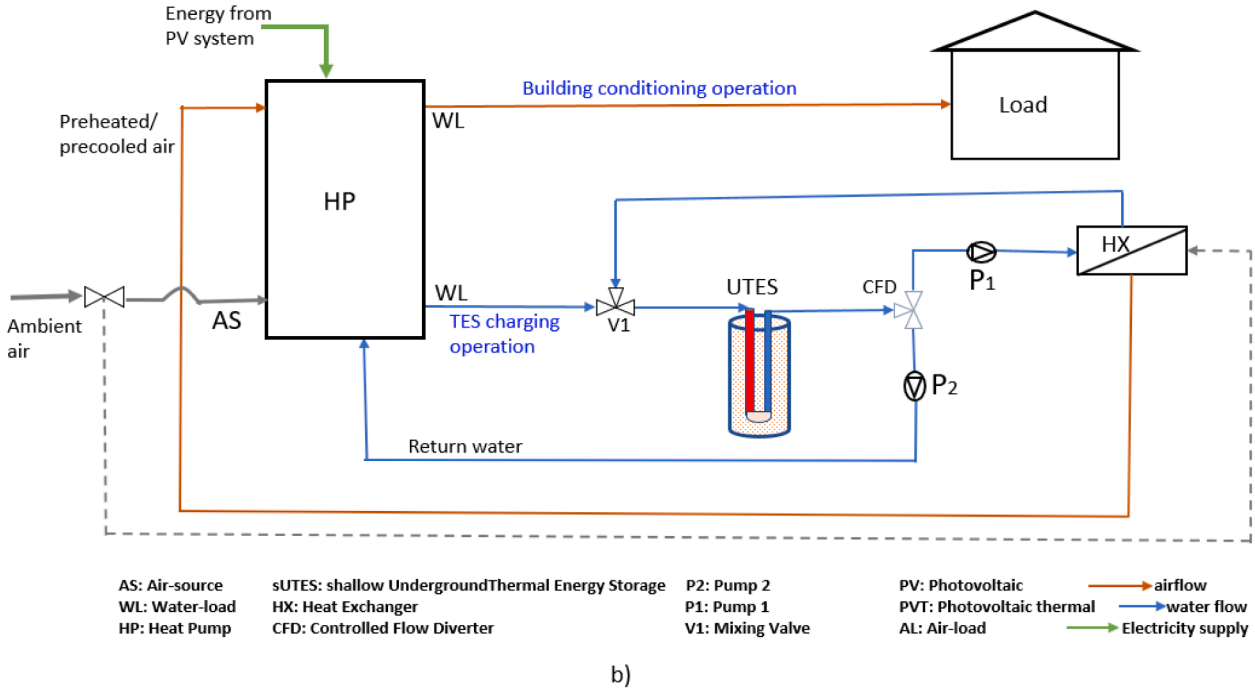

Fig. 2. a) Building energy demand and supply b) Proposed System Configuration.

$$If\ P2H(t_{i-1}) = ON/OFF \begin{cases} P2H(t_i) = ONif E_{pv,surplus} > 0 \\ P2H(t_i) = OFFif E_{pv,surplus} < 0 \end{cases} \quad (2)$$

Where P2C and P2H signals operate at the timestep, t_i as a function of the previous timestep, t_{i-1} and $E_{pv,surplus}$ is the surplus energy from PV production after accounting for the base and plug-load and the designed electric consumption of the heat pump. The control method of this study maintains the initial and final temperature of the UTES to approximately the same by adjusting the start time of P2C and P2H, respectively, using trial-and-error approach. This is important since it contributes largely to maintaining the annual thermal balance of soil temperature in the UTES. In addition, this approach could contribute to the cases of thermal imbalance of ground-source heat pumps when the heating and cooling demand is not balanced.

2.4. Description of simulation models

The system configurations representing the conventional and test systems were modeled in the TRNSYS simulation tool, combining various components to ensure stability, controlled operation, and performance evaluation of key parameters from the essential components. Two cases were modeled for evaluation:

Case 1: This case consists of an ASWL heat pump with P2HC operation using shallow UTES (sUTES) of 1.5 m deep with insulation on the top and sides of the storage volume, and source-supply configuration as shown in Fig. 3 b). The source-supply configuration implies the use of thermal energy from the sUTES to preheat and precool the air supply to the source side of the heat pump during winter heating and summer cooling, respectively. During the heating

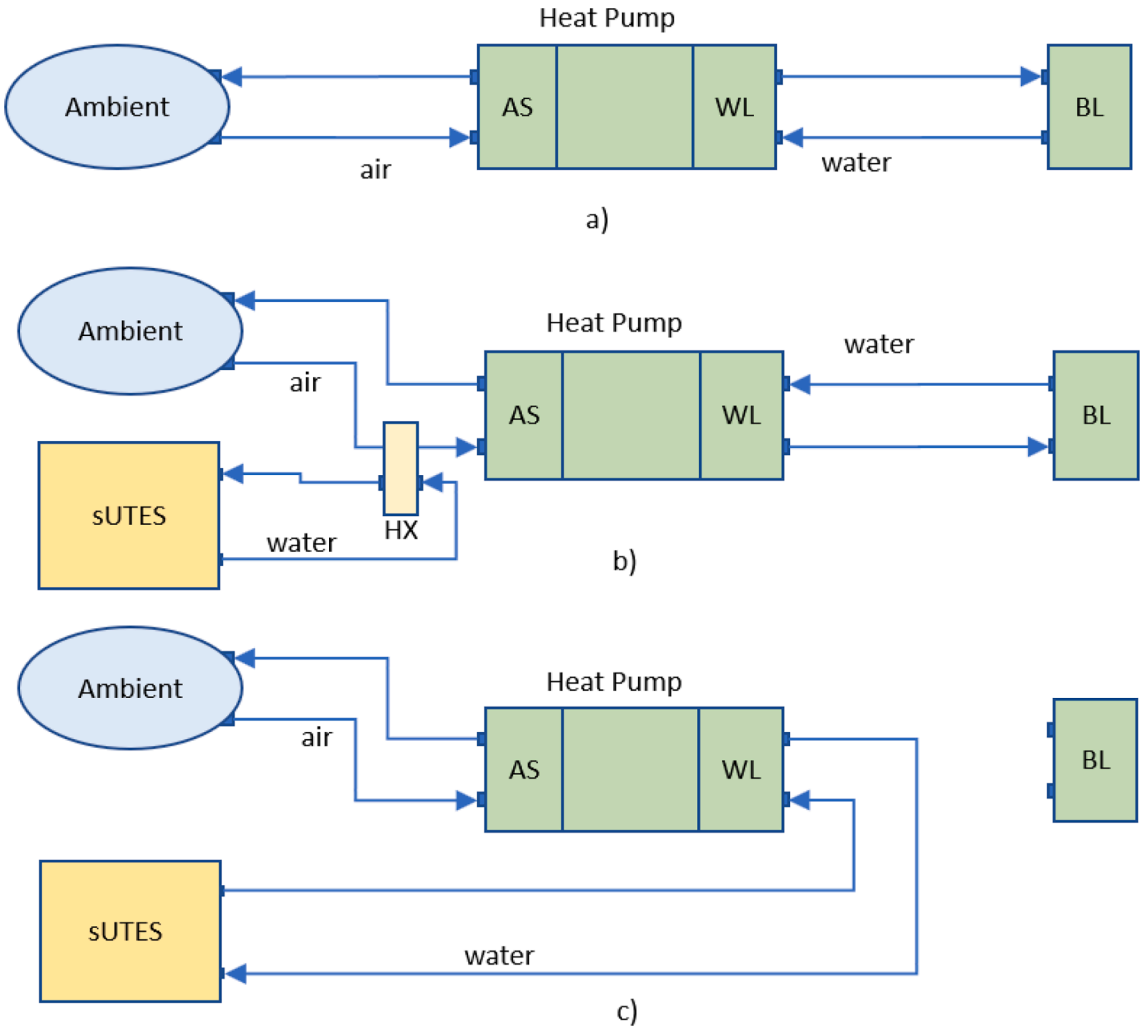

Fig. 3. CASE 1. a) Conventional case with no P2HC, b) Test case 1 with sUTES for summer and winter space conditioning operation mode, and c) case 1 test case with sUTES for spring and autumn operation mode with P2HC.

and cooling seasons, the heat pump functions as a dual-source with air and sUTES. employed for heating and cooling operations, while P2HC is employed for the charging of the shallow UTES. A reference model, as shown in Fig. 3 a), was developed for performance evaluation.

Case 2: This case consists of an ASWL heat pump with 150 m deep UTES and P2HC operation as the test case. The reference study scenario in Case 1 is used for evaluation.

For all the cases, a buffer tank (BT) is placed between the load side of the heat pump and the building load to modulate the thermal energy supplied to the load. The water flow rates for the UTES, heat pump, and buffer tank were set as 300,000 kg/h. The water side of the heap pump was set to operate for a maximum temperature of 50 °C during the heating period and 5 °C during the cooling period. In the same manner, the average temperature of the buffer tank was maintained between 50 °C in winter and 5 °C in summer using the same flow rate. It is worth noting that the shallow and deep underground UTES systems have been designed with the same volume in this study but differ in their number of boreholes and depth.

2.4.1. Solar photovoltaic model

The solar PV system, as represented in Fig. 2 a) produces the energy required for heating and cooling and some percentage of the other electrical energy demand (baseload and plug-load) in the building and its surplus in spring and autumn used for P2HC operation. It is represented in TRNSYS with the Type50 component from the TESS library (see parameter details in Table 1) with losses as a function of temperature, windspeed and geometry [41]. The PV area of 2,500 m^2 was chosen to meet at least 30 % of the roughly expected total energy consumption of the building at 21 % module efficiency. This area is based on available rooftop area for PV module installation on the actual target building where the annual electric load was measured. This model leverages the available area on the building for installation of 21 % PV modules for analysis hence, the detailed sizing pertaining the DC-AC inverters and the modeling of the PV output variables are not considered in detail.

2.4.2. Building thermal load model

A typical school building, considered an effective and simple building thermal model for space heating and cooling demand, was modeled using the lumped capacity (Type88) model from the TESS library. The detailed parameter description, shown in Table 1, provides a comprehensive understanding of the building's characteristics. The building comprises a total of 2,500 m^2 rooftop area through which PV panels can be installed. The parameters, such as the building loss coefficient and building capacitance used for the simulation, were determined using equations (5) and (6) to correspond to the cooling and heating loads of 26.27 kWh/m^2 and 52.69 kWh/m^2, respectively, which are typical for public school buildings in different regions [42]. This building model was selected for simplicity, and it consists of four floors, each with a total

Table 1
System Components and parameters.

Parameters	Value	Units
Solar PV		
Module area	2,500	m^2
Collector efficiency factor	0.7	–
Fluid Thermal Capacitance	4.19	kJ/kg·K
Collector plate absorptance	0.9	–
Number of glass covers	1	–
Collector plate emittance	0.9	–
Loss coefficient for bottom and edge losses	20	kJ/ hr·m^2·K
Collector slope	45	degrees
Extinction coefficient thickness product	0.03	–
Temperature coefficient of PV cell efficiency	−0.0003	1/K
Temperature for cell reference efficiency	20	C
Packing factor	0.5	–
Building Model		
Building loss coefficient	6.0	kJ/ hr·m^2·K
Total building capacitance	783,125	kJ/K
Specific heat of building air	1.007	kJ/kg·K
Density of building air	1.2	kg/m^3
Total surface area per building floor through which thermal losses occur	1312	m^2
Total rooftop area available for PV installation	2500	m^2
The total volume of the building per floor	4500	m^3
Humidity ratio multiplier	10	–
Initial temperature	20	C
Initial humidity ratio	0.005	–
Latent heat of vaporization	2260	kJ/kg
Underground Thermal Energy Storage		
Storage Volume	800	m^3
Borehole Depth for shallow UTES	1.5	m
Borehole Depth for deep UTES	150	m
Header Depth	0.5	m
Number of Boreholes (shallow)	1386	
Number of Boreholes (deep)	14	
Borehole Radius	0.102	m
Storage Thermal Conductivity	15.975	kJ/hr·m·K
Storage Heat Capacity	5950.01	kJ/m^3/K
Outer Radius of U-Tube Pipe	0.016	m
Inner Radius of U-Tube Pipe	0.012	m
Center-to-Center Half Distance	0.05	m
Fill Thermal Conductivity	2.50	kJ/hr·m·K
Pipe Thermal Conductivity	11.149	kJ/hr·m·K
Reference Borehole Flowrate	3.0×10^5	kg/hr
Fluid Specific Heat	4.19	kJ/kg·K
Fluid Density	1000	kg/m^3
Insulation Thickness	0.2	m
Insulation Thermal Conductivity	0.2001	kJ/hr·m·K
Initial Surface Temperature of Storage Volume	17	°C

external surface area of 1,312 m2 through which the thermal losses take place. Each floor has its own heat pump, with the heat pump serving the first floor used for evaluation, while the second, third, and fourth floors each consist of conventional ASHPs. In this building model, the effects of the ambient conditions, such as the air temperature, humidity ratio, percentage humidity ratio, rate of infiltrating air, as well as latent heat gains, were considered. The equation for the energy balance of the building zone is shown in Equation (3) [41]. The zone conditioning signal maintains the room temperature between 18 °C and 22 °C during the heating period and between 24 °C and 28 °C during the cooling period to account for an operating deadband of 4 °C and 4 °C for the heating and cooling seasons, respectively. The building is assumed to be airtight, implying a negligible infiltration mass flow rate, as discussed by Emmerich et al. [43] and Mathur and Damle [44]. This corresponds to a negligible heat flow, $Q_{infiltration}$. The rate of energy gain by lighting and the rate of sensible energy gain by people are assumed to be 5 kW and 10 kW, respectively, per floor. Using this building model, the pre-determined heating and cooling loads obtained from simulation with the conventional ASWL heat pump were used for the performance evaluation of the heat pump with P2HC. This load was imposed on the liquid flow stream using the Type682 from the TRNSYS component library, such that the ASWL heat pump would meet them as required; therefore, the zone temperatures were not of the greatest importance in the study, but the met load. Consequently, an assumption was made that the heating and cooling loads were perfectly known.

$$\frac{dT_z}{dt} = Q_{hp} + Q_{ambient} + Q_{infiltration} + \sum Q_{gains} \tag{3}$$

$$Q_{hp} = \frac{\dot{m}_{hp,air} c_{p,air}}{C} \left(T_{hp,out} - T_z\right) \tag{4}$$

$$Q_{ambient} = \frac{UA}{C} \left(T_{ambient} - T_{z)}\right) \tag{5}$$

$$Q_{infiltration} = \frac{\dot{m}_{inf} c_{p,air}}{C} \left(T_{inf} - T_z\right) = 0 \tag{6}$$

Where UA represents the product of zone loss coefficient and the zone area, C is the zone capacitance, and Q_{gains} equals the heat gains from people, lights and equipment. The cooling and heating loads, $Q_{cooling}$ and $Q_{heating}$ of the building can be calculated using equations (7) and (8) as follows [41]:

$$Q_{cooling} = \int_{t_i}^{t_f} \left[\rho_{air} V_{zone} C_{p,air} \left(T_{zone} - T_{supply}\right) * Occupancy\right] dt \tag{7}$$

$$Q_{heating} = \int_{t_i}^{t_f} \left[\rho_{air} V_{zone} C_{p,air} \left(T_{supply} - T_{zone}\right) * Occupancy\right] dt \tag{8}$$

2.4.3. Electrical load demand model

The electrical load model, excluding the electricity demand for heating and cooling, includes the baseload, which is the electric load consumed continuously every 24 h, and the plug-load, which is the electricity load used by electrical appliances 10 h (8 am to 6 pm) during the weekdays. During the weekend, it is assumed that only the baseload is required. The baseload and the plug-load measured at an actual school building over a year for the study building indicate 294 MWh and 145 MWh, respectively, corresponding to a maximum of 33.6 kW baseload and 54.8 kW plug-load [45]. This demand and consumption were modeled using the Type516 from the TRNSYS component library. Fig. 4, shows the pre-determined electric power demand profile, including the building's heating and cooling demand simulated over a year and the power generation from the installed PV module. Excess PV power generation usually occurs during the spring and autumn, necessitating P2HC operations during these seasons.

2.4.4. Underground thermal energy storage model

The TRNSYS model for shallow underground thermal energy storage (sUTES), calibrated by using measured data in Eze et al. [36] was employed. The sUTES model was developed and calibrated using the Type557 component from the TRNSYS library. Using this model, a few parameter adjustments were made in terms of size to balance other load components. The sUTES system is made up of 964 boreholes with a modified volume of 800 m^3 and a depth of 1.5 m. Insulation of thickness, 0.2 m, was provided at the top and side of the storage volume to minimize thermal losses. On the other hand, the deep UTES consists of 10 boreholes with a depth of 150 m and the same volume of 800 m^3. Further specifications of the UTES are presented in Table 1. The air-source heat pump is utilized for charging the UTES during non-heating and non-cooling (spring and autumn) periods. The operational strategy is such that the cooling charge time and heating charge time can be adjusted to prevent overcharge or the supply of temperature below zero to the storage volume. This size of the system can be determined in equation (9) while its fluid-to-ground heat transfer rate during charging and discharging and its performance indicator is defined in equation (10) [41].

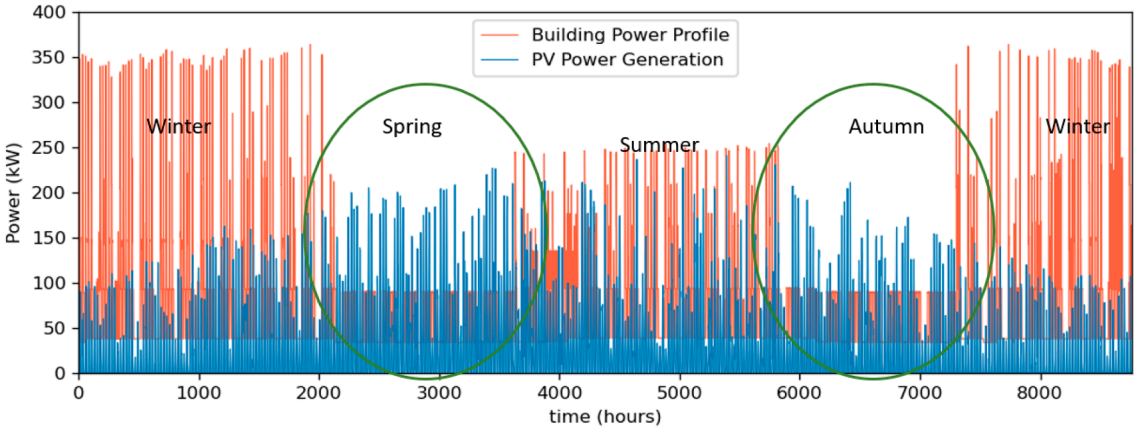

Fig. 4. Comparison of seasonal building power profile measured versus PV power generation.

$$Volume = N{*}Depth{*}\pi{*}(0.525{*}boreholespacing)^2 \tag{9}$$

$$Q_{charge/discharge} = \int_{t_i}^{t_f} \dot{m}_w C_{pw}(T_{in} - T_{out})dt \tag{10}$$

2.4.5. Heat pump model

The heat pump functions as both a dual source of air and water, as shown in Fig. 2 b). Therefore, a reversible Air-to-water HP of Type941 from the TRNSYS component Library was chosen to model the ASWL, case 1 scenario [41]. This single-stage HP can provide heated or cooled water on the load side. The heat pumps operate based on the user-specified data that is made up of the heating and cooling capacities, as well as their power consumptions, which are functions of the air flow rates, water flow rates, and the water supply temperature. In this study, the cooling and heating performance data, as provided by the manufacturer, was used. During spring and autumn, it operates using ambient air as the air source heat pump, while in summer and winter, it utilizes stored cool and warm energy from UTES to precool and preheat the ambient air using a water–air heat exchanger on the air source side. The heat pump specifications include 160 kW heating and cooling capacities, with 40 kW and 50 kW power consumption for cooling and heating, respectively. The rated air and liquid flow rates are 10,000 l/s and 300,000 kg/hr, respectively. A heat pump of these specifications was selected to adequately supply the required amount of heat to the building and sufficiently charge the thermal energy storage system. Performance evaluation of the air and water side of the HP was based on the mathematical reference for the energy balance and the coefficient of performance (COP) as shown in Eqn 11, 12 and 13 for cooling and heating operation from the initial start time, t_i to the final stop time, t_f for the specific operation period or season.

$$Q_{cool/heat} = \int_{t_i}^{t_f} \dot{m}_w C_{pw}(T_{in} - T_{out})dt \tag{11}$$

$$Q_{cool/heat} = \int_{t_i}^{t_f} \dot{m}_a C_{pa}(T_{in} - T_{out})dt \tag{12}$$

$$COP_{cool/heat} = \frac{Q_{cool/heat}}{\int_{t_i}^{t_f} (E_{com} + E_{fan})dt} \tag{13}$$

Where E_{fan} represents the total power of the fan and E_{com} represents the compressor power.

2.4.6. Heat exchanger model

A 4 kW heat exchanger with air and water flow rates, 10,000 l/s and 300,000 kg/hr, respectively, as with the heat pumps, was used in the system to convert heat energy in water from thermal storage to air flowing into the source-side of the heat pump and vice versa. In summer, a constant effectiveness Type699 heat exchanger was used to precool the inlet air to the heat pump. This heat exchanger automatically bypasses the hot side liquid to maintain the cold side air temperature set at 13 °C based on the minimum allowable air inlet to the heat pump. Similarly, a Type 652 constant effectiveness heat exchanger was used during the heating season. In this type of heat exchanger, the hot-side water fluid is bypassed to maintain the cold-side outlet air fluid temperature set at 25 °C based on the maximum allowable air temperature to the heat pump during the heating period. These allowable air temperatures were defined based on the heat pump performance data. These control strategies aim to regulate the temperature of the air that is preheated or precooled within acceptable limits before supply to the heat pump. The heat exchanger effectiveness value was set to 0.85, and the conventional heat capacities of water and air, 4.19 kJ/kg·K and 1.02 kJ/kg·K, respectively, were used.

2.5. Model validation and constraints

Prior to modeling the system configuration in this study, the major component models were validated for performance reliability. These include the UTES, heat pump, building load, and the PV system. Among these, the UTES and heat pump are key components for evaluation. The shallow UTES system was previously modeled and calibrated using field experimental data by Eze et al. [36]. The validation of this model in the prediction of the outlet water temperature achieved a root mean square error (RMSE) of 0.94 °C and a coefficient of variation of the RMSE of 3.16 %, which is within the acceptable error for application. Further detail is provided in the supplementary reference. Similarly, the heat pump's performance was based on normalized heating and cooling performance data provided by the manufacturer under test conditions for the air-to-water heat pump [46]. This performance data is available in the supplementary reference (Table A- 7 to A-9) of this study. The cooling performance data, specifies water inlet temperatures between 5 °C and 15.6 °C, and inlet air temperatures between 12.78 °C and 38 °C. For the heating performance, the data covers inlet water temperatures from 30 °C to 55 °C and inlet air temperatures from −20 °C to 25 °C. The heat pump model is constrained to operate within these ranges of natural variables, which defines its effective operating conditions. Beyond these data ranges, the maximum or minimum cooling performance values are returned since the model does not extrapolate, hence the ranges were adequately maintained in the simulation for reliability. Additionally, a simple model for the building load using measured data over a year for the base-load and plug-load in the target building was applied. This approach lends credibility to the model by grounding it in real usage patterns. The building thermal load model was designed to fall within the typical annual heating and cooling load range for school

buildings: 52.69 kWh/m2 for heating and 26.27 kWh/m2 for cooling [42], followed by the design of the PV system to cover the actual measured rooftop area of 2,500 m^2 of the case study building.

The methodology in this study has been widely applied in previous research for modeling and simulating energy systems and processes without the physical construction of the system configuration for further verification. For example, Emmi et al. [47] performed a TRNSYS simulation study that included a solar PVT model, hot water tank, water-to-water heat pump (WWHP), air-to-water heat pump (AWHP), ground-source heat pump (GSHP), and building thermal load. The authors modeled the heat pumps using manufacturer-provided performance data. Yang et al. [48] simulated a system configuration consisting of solar collectors, thermal storage tanks, and heat pump models (Type668 and Type941 in TRNSYS) using manufacturer-provided heating and cooling performance data. Similarly, Pelella et al. [49], Liravi et al. [50], and Wang et al. [51] performed simulation studies of heat pumps combined with components such as thermal storage, solar energy systems, and building load models using manufacturer-provided efficiency data for the heat pumps. Furthermore, Liu et al. [52] developed a novel concept that integrates absorption heat pumps and carbon capture technology. The proposed system configuration was modeled and evaluated against a conventional case without the integrated heat pump using key performance indicators. The study did not construct the physical system assembly for verification but rather evaluated the performance by the efficiency of each component.

This brief literature review justifies the methodology employed in the present study. Simulation studies have been widely conducted in previous research to evaluate the impact of new or improved components on system configurations. These studies typically involve creating a model of the system with the proposed changes and comparing its performance to a baseline model without the modifications while mimicking the actual system designs. In scenarios where the physical construction of all component models is resource-intensive, system performance validation can be based on manufacturer-provided test condition data. Overall, the present study is valid, and the obtained results in comparing the system configuration with and without P2HC operations are reliable based on the validation of the component models and the use of manufacturer-provided performance data for the heat pump model.

2.6. System performance measures

In this study, six performance indicators were used for the evaluation of overall system performance during space heating, space cooling, and P2HC operation. First is the surplus energy utilization ratio (SEUR) defined in Eqn 14. This is the ratio of the total PV electricity consumed for P2HC operation, ($E_{PV,P2HC}$) from the test case of case 1 and case 2 to the total surplus electricity that exists on an annual basis, ($E_{surplus}$) from the base case. Where $E_{surplus}$ is the difference between the total PV power generation per year, $E_{PV,total}$ and the total PV power consumed, $E_{PV,used}$ over the year. The $E_{PV,used}$ is the total PV electricity that is consumed by the building, which includes the power consumption of the heat pumps during winter heating and summer cooling ($E_{PV,HnC}$), and the base electricity consumption ($E_{PV,etc}$) which includes other building electricity demands, including lighting and water pumps, in the system configuration. This performance index explains the percentage of the surplus energy utilized for power P2HC operation instead of being wasted or exported to the grid. It improves the economic benefit by increasing savings.

$$SEUR = \frac{E_{PV,\ P2HC}}{E_{PV,\ surplus}} \times 100 \tag{14}$$

Where mathematically $E_{PV,surplus} = E_{PV,total} - E_{PV,used}$.

The second performance indicator is the self-consumption ratio (SCR). This is defined in Eqn 15, as the ratio of the PV electricity utilized in the building for not only meeting the building's electricity demand but also charging the ground thermal storage by the heat pump for P2HC, $E_{PV,used}$ to the total PV electricity generated, $E_{PV,total}$. This indicator is necessary to provide insight into the total PV power generated that is directly consumed on-site. By maximizing this ratio, dependency on the grid is reduced, and the return on investment of the PV project is improved with a reduced payback period.

$$SCR = \frac{E_{PV,used}}{E_{PV,\ total}} \times 100 \tag{15}$$

The third performance indicator is the power-to-heat/power-to-cool (P2HC) efficiency defined in Eqn 16. In this performance evaluation, the energy saved through P2HC implementation for winter heating and summer cooling and the excess PV electricity utilized for P2HC operation via UTES were considered. Therefore, it is defined as the ratio of the difference between the energy consumption of the heat pump for the conventional case during heating and cooling, E_{conv} and the energy consumption by the heat pump for the test case during heating and cooling, E_{test} to the energy consumption by the heat pump during power-to-heat and power-to-cool (UTES charging) operation, E_{p2hc}. This performance indicator maximizes savings and improves the profitability of P2HC operations.

$$P2HC\ efficiency = \frac{\left[\int_{t_i}^{t_f} E_{conv}dt - \int_{t_i}^{t_f} E_{test}dt\right]_{cooling/heating}}{\left[\int_{t_i}^{t_f} E_{p2hc}dt\right]_{charging}} \times 100 \tag{16}$$

Heat pump energy saving was also defined as the fourth performance indicator in this study. It is defined as the ratio of the difference between the total energy consumption of the heat pump over heating and cooling timesteps for the conventional case, E_{conv} and the energy consumption of the heat pump over heating and cooling timesteps for the test case, E_{test} to the total energy consumption of the heat pump over heating and cooling timesteps for the conventional case, E_{conv} as shown in Eqn 17. This indicator quantifies the energy saved by using the energy stored in the UTES to preheat and precool the inlet air to the heat pump. It indicates how the P2HC operation improves the heat pump's performance.

$$Energy savings = \frac{\left[\int_{t_i}^{t_f} E_{conv}dt - \int_{t_i}^{t_f} E_{test}dt\right]_{cooling/heating}}{\left[\int_{t_i}^{t_f} E_{conv}dt\right]_{cooling/heating}} \times 100 \tag{17}$$

Seasonal coefficient of performance (SCOP) was also defined for the heat pump in Eqn 18 as the fifth performance indicator. It is the ratio of the total heat transfer rate for a specified season defined previously in equation (9), Q_{season} to the total power consumption of the heat pump, $(E_{com} + E_{fan})_{season}$ for the specified season. This indicator quantifies the seasonal improvement in the efficiency of the heat pump. It is an average value that accounts for temperature fluctuation and operating conditions throughout the year. Since the heat pumps operate differently at various outdoor temperatures, SCOP captures these variations, offering an accurate performance measure across seasons.

$$SCOP = \frac{Q_{season}}{\int_{t_i}^{t_f} (E_{com} + E_{fan})_{season} dt} \tag{18}$$

Finally, the sixth performance indicator was defined for both shallow and deep UTES. The total thermal efficiency, η_{th} is defined as the absolute values of the ratio of the total heat extracted from the UTES for heating and cooling during winter and summer, $\left|\int_{t_i}^{t_f} \dot{Q}_{d,winter}\right| + \left|\int_{t_i}^{t_f} \dot{Q}_{d,summer}\right|$ to the absolute values of the total heat injected into the UTES for its charging during spring and autumn, $\left|\int_{t_i}^{t_f} \dot{Q}_{c,spring}\right| + \left|\int_{t_i}^{t_f} \dot{Q}_{c,autumn}\right|$ in Eqn 19, where subscripts d and c represent discharge and charge, respectively. This performance indicator is crucial

as it determines how effectively the stored thermal energy is recovered and utilized for the building space conditioning.

$$Thermalefficiency, \eta_{th} = \frac{\left|\int_{t_i}^{t_f} \dot{Q}_{d,winter}\right| + \left|\int_{t_i}^{t_f} \dot{Q}_{d,summer}\right|}{\left|\int_{t_i}^{t_f} \dot{Q}_{c,spring}\right| + \left|\int_{t_i}^{t_f} \dot{Q}_{c,autumn}\right|} \quad (19)$$

3. Results and discussion

In this section, the results obtained from the analysis of the system configuration with its operational strategy guided by the simple control methods are analyzed and discussed. For case comparison, some basic requirements were followed: first, the P2C or P2H beginning period is adjusted to ensure that the average initial temperature of the ground at the beginning and final temperature at the end of the simulation period remains approximately the same. Secondly, the P2C beginning time for cases 1 and 2 are exactly the same, however, the P2H period can be adjusted to maintain approximately the same initial and final average temperatures of the ground. Finally, the heat supply from buffer tank to meet the imposed load for all cases are ensured to be approximately the same. These conditions are also applied during the performance of the parametric analysis.

3.1. Case 1

The study utilized shallow underground thermal energy storage (sUTES) in combination with an existing air-source heat pump, implementing an operational strategy to efficiently store and extract thermal energy from the ground. Fig. 5 illustrates the system's performance for case 1, showing the inlet and outlet temperatures (Tutes_in and Tutes_out) of the sUTES, as well as ground temperature variations. These variations are represented by the average storage temperature (Tutes_ave_test), the average soil temperature at the center of the borehole (Tutes_center_test), and the average soil temperature at the edge of the borehole (Tutes_edge_test). The system demonstrated its effectiveness by extracting heat energy from the ground during both winter and summer seasons, thereby improving the heat pump's performance for heating and cooling application.

3.1.1. Performance of shallow underground thermal energy storage for case 1

Fig. 5 a) demonstrates that when pump P1 is switched on to generate flow between the sUTES to HX at the source side of the heat pump, the outlet water temperature from the sUTES exchanges heat with the inlet air, resulting in preheating or precooling the air to a more efficient temperature during space cooling and heating periods. As a result, the returned water temperature from HX to the sUTES drops during the winter heating between 0 h and 2160 h and between 7296 h and 8760 h. Similarly, the returned water temperature from HX to the sUTES increases during the summer, cooling between 3624 h and 5832 h. In this analysis, the operational dynamics of an ASWL heat pump in combination with a PV system are examined for their role in charging the sUTES system. The spring P2C operation started on April 1, at the 2160 h of the year, and ended on May 31. Similarly, the autumn P2H operation began

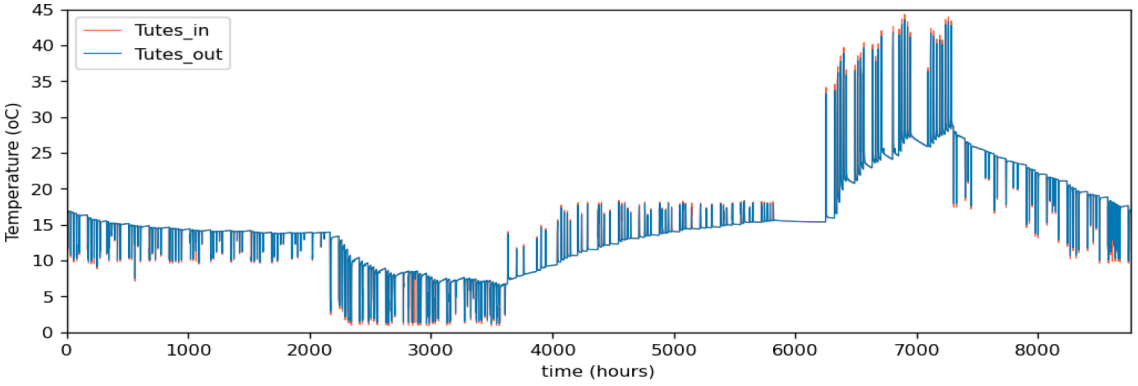

a)

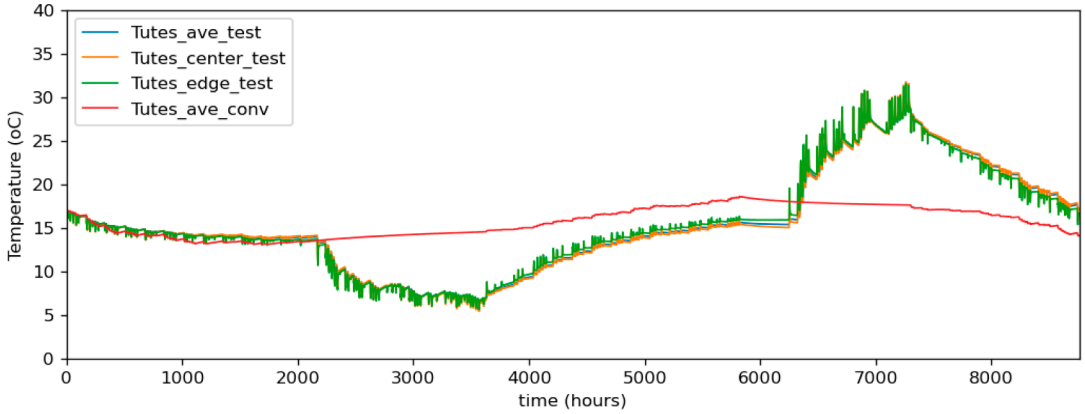

b)

Fig. 5. Temperature variation sUTES for CASE 1 a) Inlet and outlet temperatures b) Ground temperatures.

on September 1 at 6220 h and ended on October 31. These periods were chosen to provide sufficient heat required to cool or heat the ground to a suitable temperature for cooling or heating purposes. The P2C or P2H periods are adjusted to satisfy condition that the average initial and final ground temperatures must remain approximately the same at the beginning and end of the simulation. This strategy can mitigate the tendency to supply the working fluid to the ground at a freezing temperature, especially without an adequate control method. Additionally, in the case of insufficient surplus energy, the flexibility in adjusting this charging duration will provide a solution to utilizing the available effectively. During the spring charging phase, characterized by cooling requirements, the ASWL heat pump leverages excess electricity generated by the solar PV to attain a discharge temperature of approximately 2 °C. This low working fluid temperature is then used to charge the sUTES in P2C operation mode. Conversely, in the autumn P2H operation mode, the heat pump supplies the sUTES with a temperature of around 50 °C to charge the storage volume effectively. The temperature difference between the inlet and outlet temperature of the UTES can be observed, indicating a significant fluid-to-ground heat transfer.

The result of the average temperature of the sUTES, denoted as Tutes_ave_test, is graphically represented in Fig. 5 b). It indicates a charging temperature reaching approximately 8 °C from around 15 °C during spring P2C operation and ascending to about 25 °C from around 15 °C in autumn P2H operation, in contrast to the conventional case, whose Tutes_ave_conv remained between 15 °C and 17 °C, signifying an improvement in the test case. This temperature dynamic trend was also followed by the results of the temperature at both the center (Tutes_center_test) and periphery (Tutes_edge_test) of the UTES, revealing spring charging temperatures around 5 °C from around 15 °C and autumn values near 32 °C from around 15 °C. Notably, during the winter and summer seasons, there is a tangible heat exchange between the fluid from the sUTES and ambient air within the heat exchanger. This preheated or precooled air is then supplied to the source side of the heat pump. Similar heat exchange phenomena are observed in spring, with heat flow from the ground to the working fluid, and in autumn, where the reverse occurs. The sUTES thermal efficiency was quantitatively evaluated using Eqn 19, yielding an efficiency rate of 60 %. The heat loss during the spring and autumn P2C and P2H operations were calculated as 4961.53 kW and 6042.41 kW, respectively, with most of the heat loss attributed to the bottom of the storage volume without insulation.

3.1.2. *Cooling and heating performance of the heat pump for case 1*

In this study, the dual functionalities of the heat pump were employed. Fig. 6 presents a comparative analysis of inlet temperatures of air to the source side of heat pump for both conventional and test configurations cases with test Case 1 which means the source side of the heat pump is precooled and preheated by shallow UTES. In conventional operation, during severe winter conditions, the heat pump receives air at temperatures as low as −15 °C for its heating function. Conversely, in summer, it is exposed to temperatures reaching 35 °C for cooling. The test case, however, demonstrates a significant modification in these temperature ranges due to the integration of air pre-heating and pre-cooling through the sUTES P2HC operation during heating and cooling periods, respectively. Specifically, for heating, the inlet temperature of the source side of the heat pump was increased from −15 °C to near a maximum of 19 °C, and for cooling, it was decreased from 35 °C to near a minimum of 13 °C. This action is depicted more explicitly in Fig. 7, which shows a one-week period of air temperature preheating and precooling. Consequent to this, significant improvement in the power consumption of the heat pump was observed, as shown in Fig. 8. The power consumption during the heating period from November to March was more for the conventional case, similar to the cooling period from June to August. Additionally, the power consumption during the spring P2C operation in April and May and autumn P2H operation in September and October was shown.

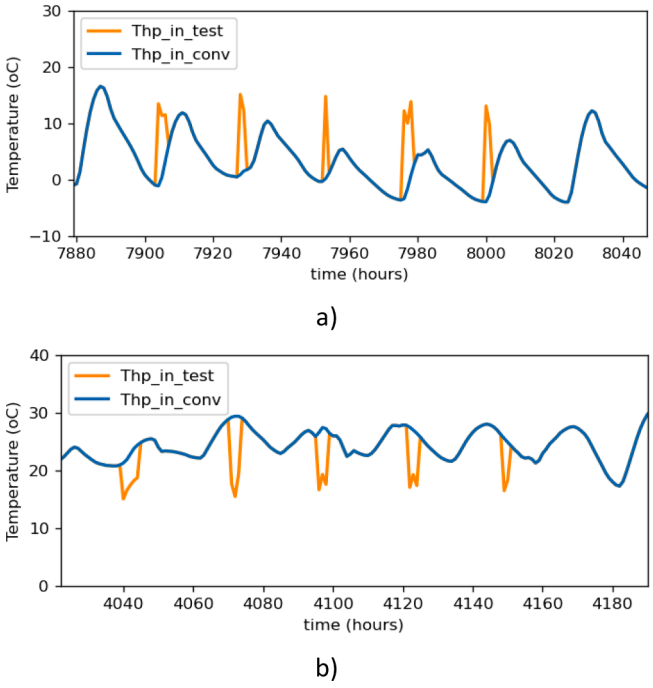

Fig. 7. Case 1 one-week view of inlet air temperature to the source side of heat pump for conventional and test cases a) preheating operation in space heating mode and b) precooling operation in space cooling mode.

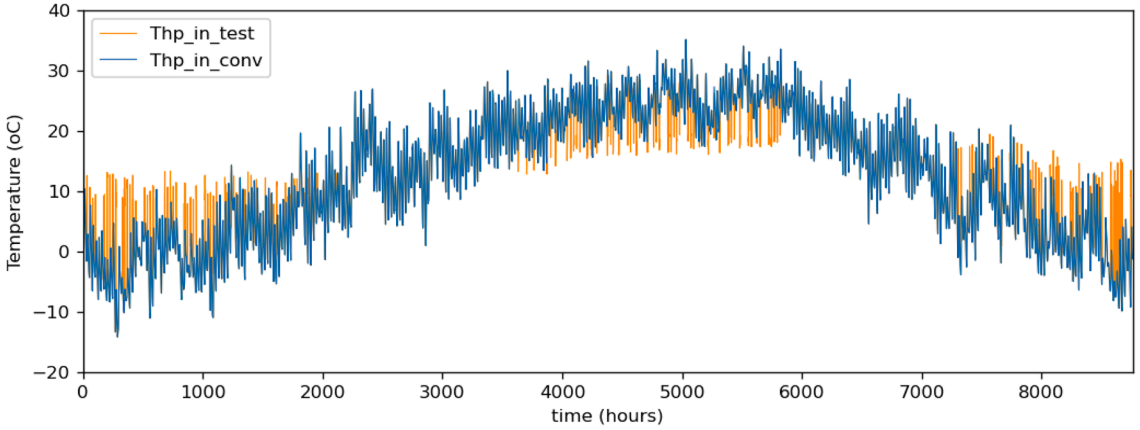

Fig. 6. Case 1 inlet air temperature to the source side of heat pump for conventional and test cases.

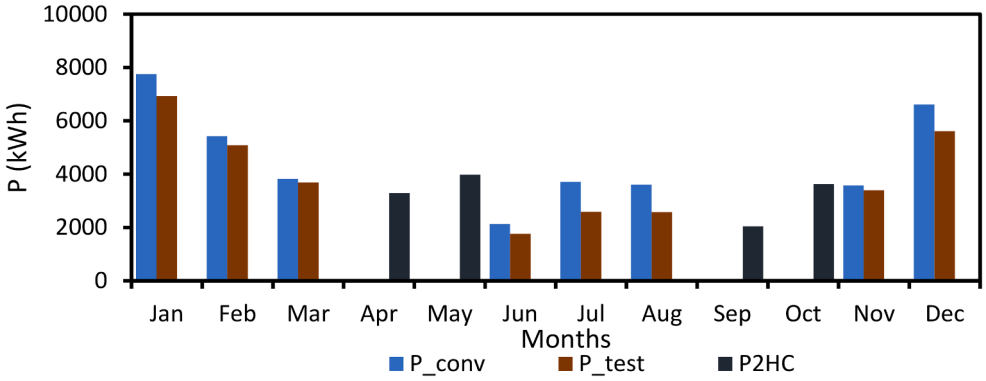

Fig. 8. Comparison of monthly power consumption of heat pump for conventional and test case for Case 1, including during P2HC operation.

These improvements have been instrumental in modulating the air source side temperature of the heat pump, subsequently augmenting its operational efficiency. During the summer season, the SCOP showed a significant improvement, with an average COP of 6.4 for the test case, compared to the conventional case, which produced a SCOP of 4.7, as shown in Fig. 9. Similarly, during the winter season, the SCOP of 3.9 was achieved by the test case as opposed to the SCOP of 3.5 accomplished by the conventional case. Generally, a 9 % and 27 % increase in SCOP for winter heating and summer cooling was achieved from the test case compared to the conventional case.

3.2. Case 2

In case 2, a 150 m deep UTES with the same ASWL heat pump is considered for P2HC application during non-heating and non-cooling periods and for heating and cooling during heating and cooling periods. In general, case 2 study exhibited a performance similar to that of case 1, charging and discharging the UTES as well as providing the heating and cooling requirements for the building space.

3.2.1. Performance of 150 m deep underground thermal energy storage for case 2

In this case, the P2C temperature supplied to the ground from the heat pump was also limited to 2 °C and 50 °C during the P2H operation. Similar to the previous case, the present case illustrates the temperature variation of the ground as shown in Fig. 10, where the average ground temperature was lowered to 10 °C from about 17 °C during spring P2C operation and raised to 24 °C during autumn P2H operation. Similarly, the temperature at the edge and center of the 150 m deep UTES decreased to 9 °C during the spring P2C operation and increased to 28 °C during the P2H operation. This improvement as a result of the P2HC operations resulted in significant improvement similar to case 1, producing 52 % UTES thermal efficiency quantitatively evaluated using Eqn 19. The thermal losses during the spring and autumn seasons were calculated to be approximately 13325.78 kW and 16909.35 kW, respectively. This loss is attributed to the insulation lacking in this 150 m deep UTES configuration.

3.2.2. Cooling and heating performance of the heat pump for case 2

The ASWL, coupled with the 150 m deep UTES, showcased similar HP performance. The inlet temperature for the conventional case, which was as low as −15 °C in winter and around 35 °C in summer, was enhanced. In test case 2, the air temperature was raised from the lowest of around −15 °C to near a maximum temperature of 16 °C in winter and was lowered from the highest temperature of around 35 °C to temperatures between 14 and 18 °C as shown in Fig. 11. The enhancements resulted in an improved monthly power consumption in comparison with the conventional case, as shown in Fig. 12, corresponding to an increased SCOP of 3.9 during winter, compared to the 3.5 SCOP obtained from the conventional case as shown in Fig. 13. Similarly, during summer cooling, the SCOP rose to 6.2, in contrast to the conventional SCOP of 4.7. Overall, this refined method resulted in a 9 % improvement in SCOP during winter and a 23 % enhancement during summer cooling, compared to the conventional approach.

3.3. Performance Comparison of case 1 and case 2

The integrated P2HC using the UTES resulted in an improvement in the system performance for both cases. This is quantitatively evidenced by the P2HC efficiency and energy savings of the integrated power-to-heat system. Applying Eqn 16 and 17, the P2HC efficiency and energy savings were determined to be approximately 39 % and 14 %,

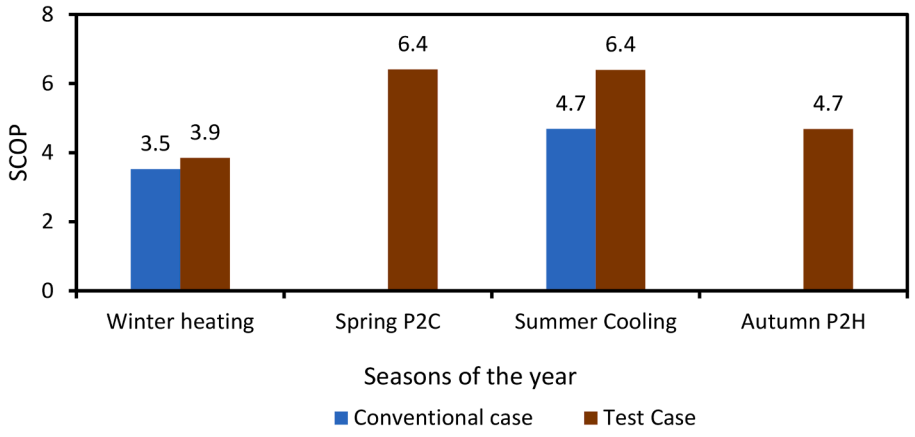

Fig. 9. Comparison of SCOP of heat pump for Case 1 with the conventional case.

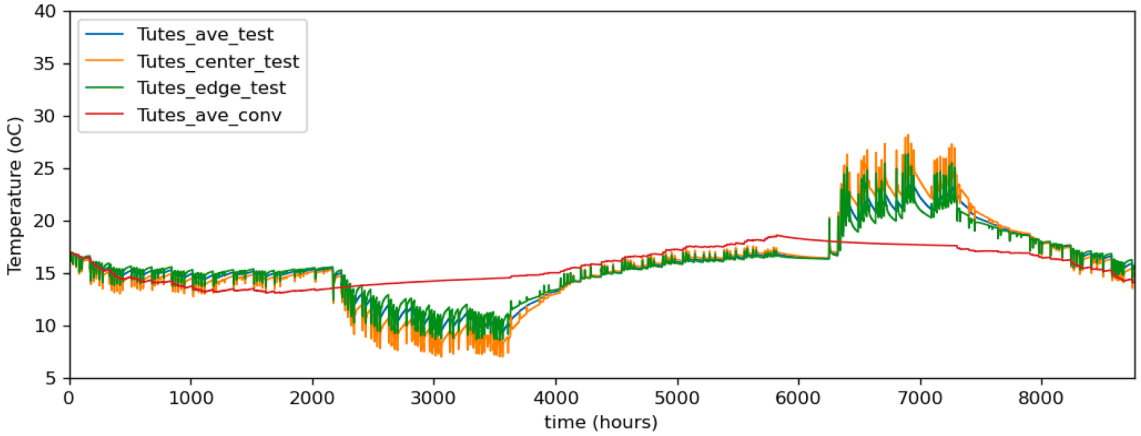

Fig. 10. Average ground temperatures for the conventional and test cases.

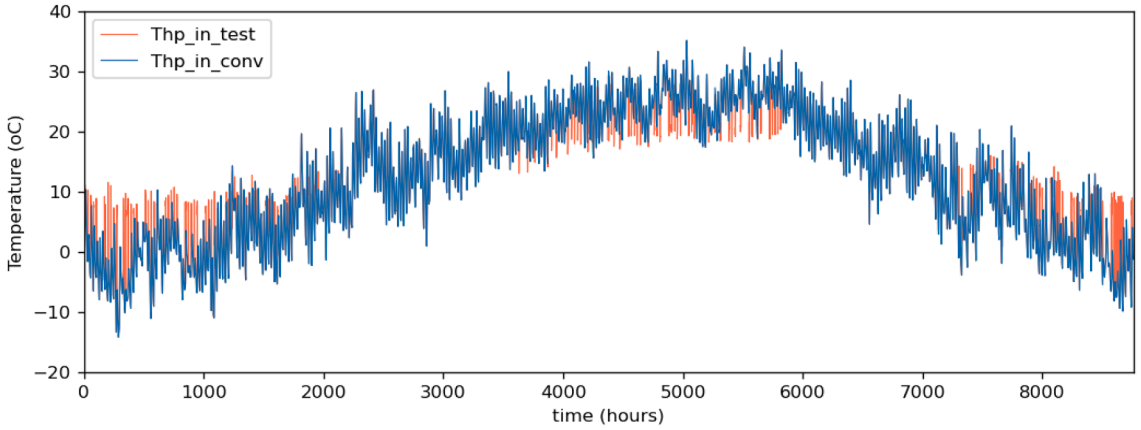

Fig. 11. Comparison of monthly power consumption of heat pump for conventional and test case for Case 2, including during P2HC operation.

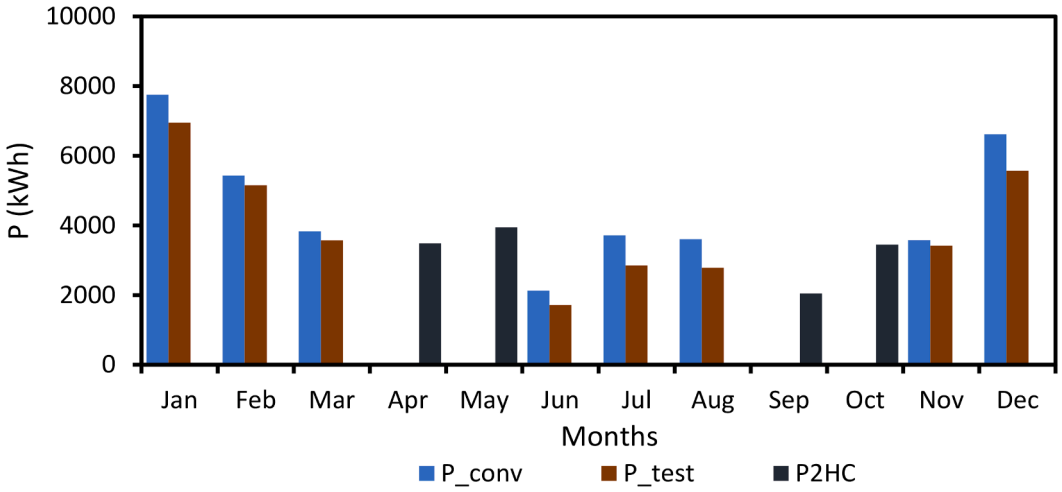

Fig. 12. Comparison of monthly power consumption of heat pump for conventional and test case for Case 2, including during P2HC operation.

respectively, for case 1. Further analysis for case 2 demonstrated a 36 % P2HC efficiency and 13 % energy savings. This performance showed a 3 % and 1 % decrease in P2HC efficiency and energy savings when compared with case 1, as shown in Fig. 14, indicating a better performance for the shallow UTES with 1.5 m depth and insulation on the top and sides of the storage volume.

The analysis depicted in Fig. 15 a) reveals that the SCR between the two cases exhibits negligible disparity, yielding an SCR of approximately 81 % in both scenarios. This result suggests that about 81 % of the PV power generated in both cases was consumed on-site. By employing P2HC operation, the test cases improved by 5 % over the conventional case, which yielded approximately 76 % SCR. Likewise, Fig. 15 b) indicates a similar SEUR for both cases, with a SEUR of approximately 26 % obtained. This finding suggests that for case system configurations,

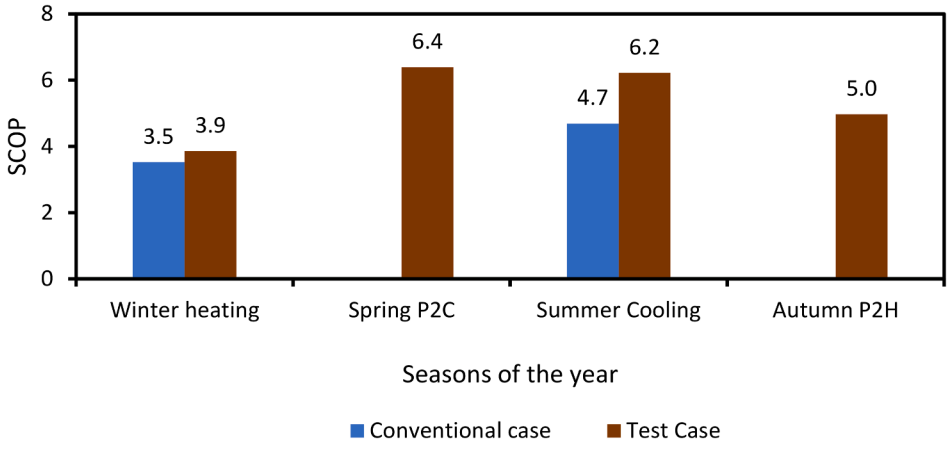

Fig. 13. Comparison of SCOP of heat pump for Case 2 with the conventional case.

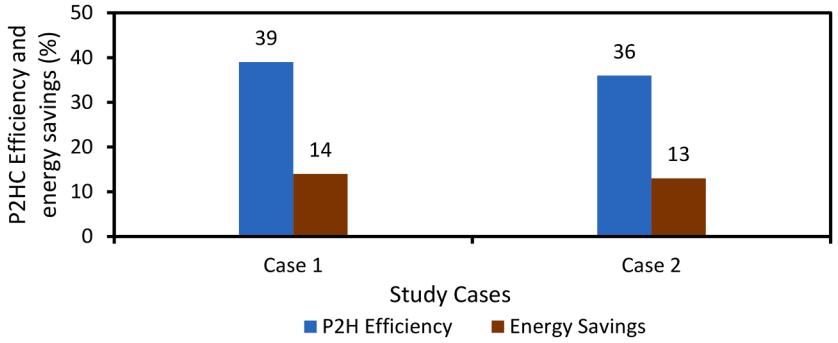

Fig. 14. Comparison of the P2HC Efficiency and Energy Savings of Case 1 and Case 2.

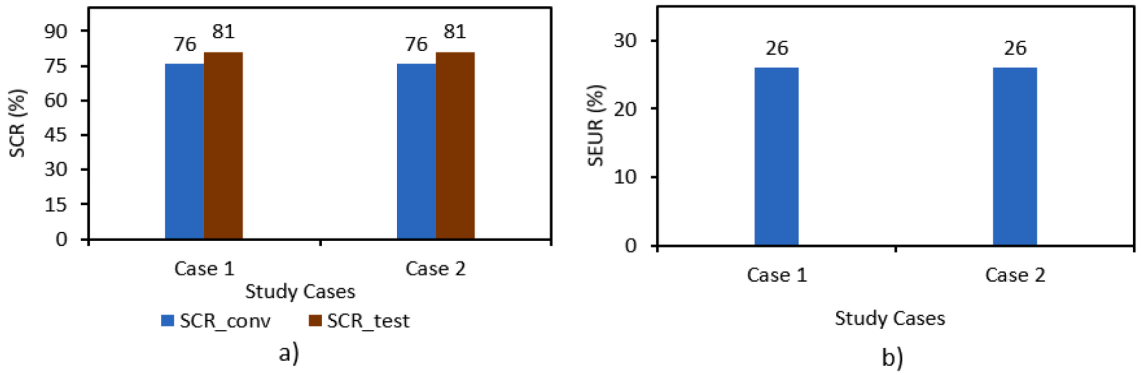

Fig. 15. a) Self-consumption ratio and b) surplus energy utilization ratio of all cases.

approximately 26 % of the surplus energy were utilized effectively in both cases for P2HC operation. The nearly identical SCR and SEUR observed across both cases may be attributed to the synchronization of P2C and P2H operation times, which commenced and concluded concurrently. Despite variations in system configurations, the synchronization likely facilitated a balanced consumption pattern, leading to consistent utilization of surplus energy. This synchronization aspect highlights a critical operational factor influencing energy consumption dynamics within the studied system configurations.

3.4. Parametric analysis

The intricate dynamics of energy systems, particularly the proposed system under study, are subject to multifaceted influences stemming from various parameters. In this section, the study undertakes a comprehensive examination of the sensitivity of the system to alterations in crucial parameters such as the UTES size, solar PV size, P2C duration, and P2H duration, with reference to the case 1 scenario. Such an analysis not only affords invaluable insights into the optimal sizing considerations for an integrated energy system but also underscores the result interaction between its constituent components.

3.4.1. Impacts of solar photovoltaic size on the system performance

The increase in solar PV size leads to a decline in UTES thermal efficiency and P2HC efficiency, although accompanied by a slight increase in the proportion of energy savings, as demonstrated in Fig. 16 a). As the PV size increases, the P2HC efficiency and the UTES efficiency converge at lower values. This implies that sizing the PV system beyond a certain

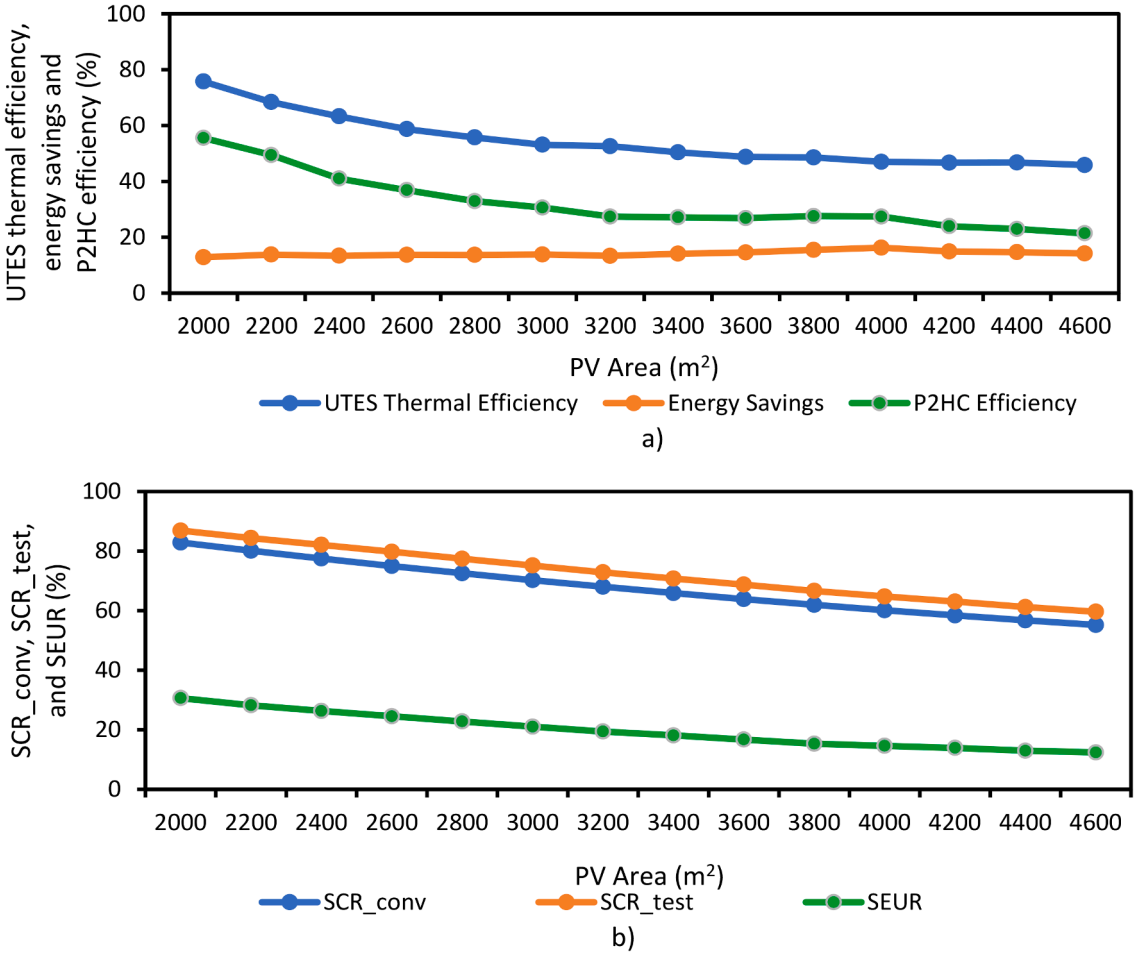

Fig. 16. Impacts of change in solar PV a) on the UTES thermal efficiency, energy savings, and P2HC efficiency, and b) on the SCR and SEUR.

size does not necessarily increase or decrease these efficiencies but would rather create a convergence to a constant lower value. However, this action may increase marginally the energy that is saved. The observed decline in the UTES thermal efficiency and the P2HC efficiency may be attributable to the fact that the more the PV size increases, the more surplus energy is generated, especially during the spring and autumn seasons when P2HC operations are scheduled to take place. Consequently, more thermal energy from the heat pump is injected into the ground, thanks to the operational strategy that allows P2HC operation to only take place in the presence of surplus energy from the solar PV system occurring in spring and autumn. As a result of this, the electricity consumption during this P2HC operation increases substantially.

Moreover, the increase in solar PV size concomitantly decreases both the Self-consumption ratio (SCR) and the surplus energy utilization ratio (SEUR). This phenomenon is demonstrated in Fig. 16 b), wherein the increase in the size of the solar PV system yields a proportional increase in surplus energy generation, consequently decreasing the SCR and SEUR. An improvement in the SCR of the test case over the conventional is also shown. As the size of solar PV increases, more power is generated, resulting in a decrease in the SCR. Similarly, the SEUR varies inversely with the surplus energy generated by the solar PV per year; therefore, the more solar PV size increases, surplus power generation is expected, which leads to the decline in the SEUR as shown in Fig. 16 b). Further details of the calculated values and the trend of the effect of PV size on the system performance is provided in supplementary material.

3.4.2. Impact of change in the size of underground thermal energy storage on the system performance

Similarly, when the size of the storage volume of the UTES changes, the system performance changes as expected. This is shown in Fig. 17. As the size of the UTES increases, the amount of thermal energy injected into the ground during P2HC operation increases, similar to the heat extracted from the ground during heating and cooling periods. Consequently, the UTES thermal efficiency increases from 57 % at a UTES volume of 100 m^3 to about 69 % at 1,420 m^3. Similarly, the P2HC efficiency increased slightly from 34 % at the UTES volume of 100 m^3 to about 43 % at 1,420 m^3, similar to the energy savings, which increased slightly from 12 % at the UTES volume of 100 m^3 to about 15 % at 1,420 m^3. This is attributed to the decrease in the power consumption of the heat pump during the heating and cooling seasons resulting from the energy supplement from the P2HC operation.

3.4.3. Impacts of change in the power-to-cool and power-to-heat durations

The P2C and P2H starting times affect the performance of the system, as demonstrated in Fig. 18. The more the charging time is postponed, the less energy is utilized for the charging operation, and the consequent thermal energy is required to lower the ground temperature. This is evident from the case of P2C operation in Spring, as shown in Fig. 18 a). The duration was postponed by 3 days (72 h) starting from April 1st, showing a significant increase in UTES thermal and P2HC efficiency. The UTES thermal efficiency was increased from 60 % at 2160 h to 68 % at 2952 h, while the P2HC efficiency was increased from 38 % at 2160 h to 53 % at 2952 h. However, energy savings fluctuate slightly between 13 % and 14 %. Similarly, adjusting the P2H operation in autumn proves

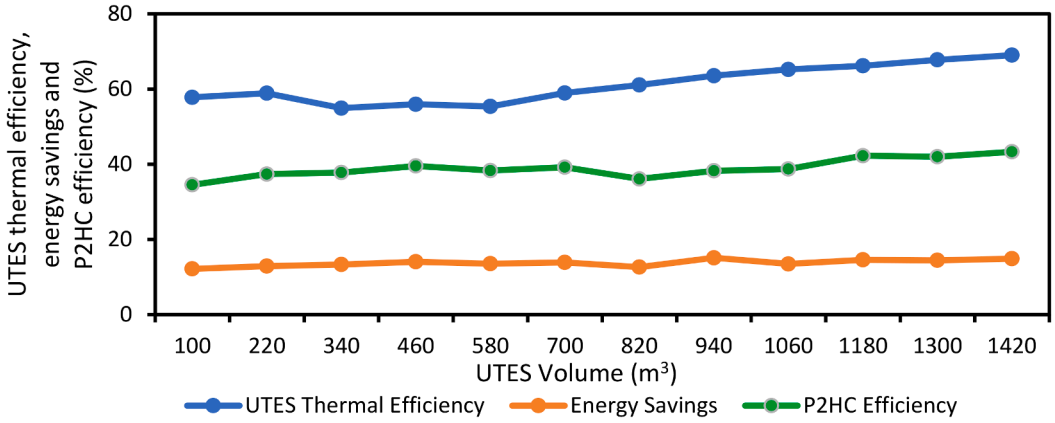

Fig. 17. Impact of change in the UTES size on system performance.

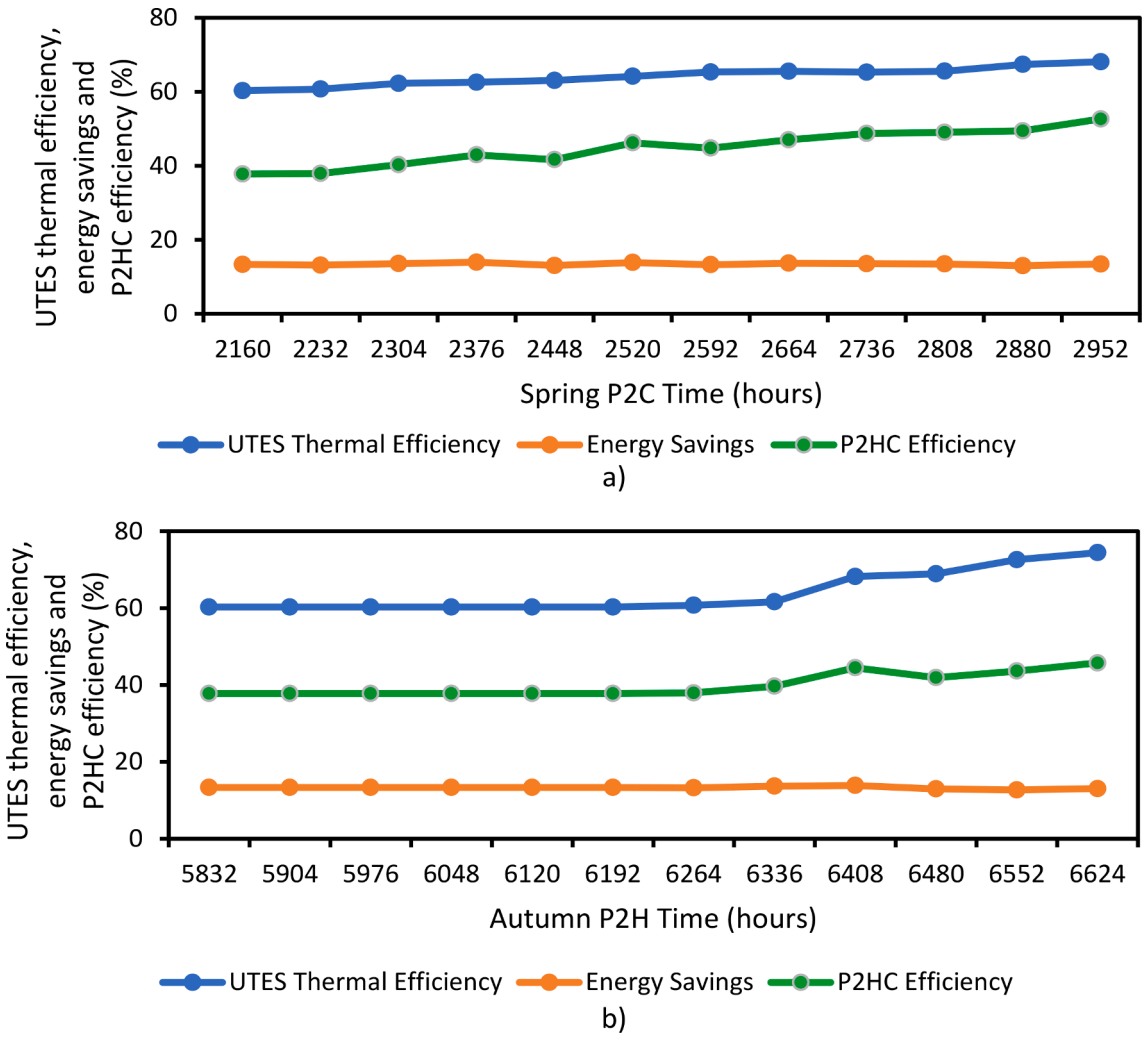

Fig. 18. Impact of the P2C and P2H starting time on the UTES thermal efficiency, energy savings and P2HC efficiency. a), spring P2C and b), autumn P2H.

equally advantageous. As depicted in Fig. 18 b), there is a notable correlation: the more P2H operation is postponed, the greater the enhancement in UTES thermal efficiency and P2HC efficiency, accompanied by a slight uptick in energy savings. This outcome mirrors the findings with the P2C operation, highlighting a common principle at play. However, the rationale behind this phenomenon differs slightly. When P2H operation is delayed, the thermal energy required to elevate ground temperature reduces, consequently increasing the UTES thermal efficiency from 60 % at 5832 h to 74 % at 6624 h and limiting electricity consumption from the surplus generation.

3.4.4. General suggestion based on the parametric analysis

The proposed system is generally sensitive to changes in various parameters, so a systematic approach is required for optimal

performance. The size of the PV reduces the UTES thermal and P2HC efficiency but slightly increases the energy savings, all to a converging point. For cost-effectiveness, this point of convergence should be the optimal size required with a factor of safety to account for unknown dynamics. Additionally, some previous studies [30,53] related the overall cost of installation of UTES, including its drilling costs, to its size; hence, for cost-effectiveness in selecting the UTES size, a moderate volume is required based on the analysis provided in this study as this tends to improve its performance. Based on the analysis, a UTES size between 800 m^3 and 1060 m^3 is suggested for use in similar system cases since the increase in the energy savings and P2HC efficiency by further incrementing the size is low. Moreover, the size in this range still keeps the UTES thermal efficiency considerably high. Further to this, the postponement of P2C or P2H increases the UTES thermal efficiency and P2HC efficiency and slightly the energy savings. Although this phenomenon is subject to the system component sizes, care should be taken to curb the issue of overcharging in the absence of control methods. It would be cost-effective to postpone both the P2C and P2H duration as was performed in this study.

4. Conclusions

In this study, a novel system configuration for the inter-seasonal self-consumption of surplus PV energy with the use of a heat pump and ground thermal storage for heating and cooling of buildings was developed and simulated. The system consists of several components, including a solar PV system responsible for supplying energy for the building's heating, cooling, and domestic hot water needs. Additionally, the UTES system is incorporated for P2HC operation, and then the heat pumps are used for both heating and cooling, along with the charging of the thermal energy storage system. Two system cases were investigated to evaluate their performance. Case 1 involves an ASWL heat pump with P2HC capabilities, functioning as a dual-source system by utilizing both air and shallow UTES insulated on the top and sides of its storage volume. Case 2 features the same ASWL heat pump with P2HC, serving as a dual-source system utilizing both air and deep UTES. A simple operational strategy was employed for its operational control over a typical year for a school building in Korea. For performance evaluation, conventional systems without P2HC operation for each of the cases were also modeled and simulated. Conclusively, parametric analysis was carried out to examine how some changes in the system parameters affect the performance of the systems for the case 1. The performance evaluation led to the following conclusions:

- Using the operational strategy, the developed system configuration could perform inter-seasonal operations. The utilization of surplus PV electricity for the seasonal P2HC strategy through the UTES was successfully performed. In spring and autumn, the heat pump used excess electricity from the PV to perform P2C and P2H operations, respectively. The dual-functionality of the heat pump was accomplished with the operational strategy. The use of a heat pump for charging the UTES and for building conditioning was achieved. During summer, the ambient air supplied to the heat pump was successfully pre-heated or pre-cooled using the thermal energy stored in the UTES. This modification significantly improved the performance of the heat pumps for all the study cases.
- The performance evaluation for the Case 1 scenario indicated that the heat pump power was reduced during the building air-conditioning operation, and consequently, the SCOP was improved. The SCOP was increased by 9 % and 27 % in winter and summer, respectively, for case 1 and 9 % and 25 % for case 2. The improvements also resulted in increased energy savings and P2HC efficiency of 14 % and 39 %, respectively. Similarly, the Case 2 scenario was improved, resulting in energy savings and P2HC efficiency of 13 % and 36 %, respectively. Cases 1 and 2 produced approximately the same SCR and SEUR, with approximate values of 81 % for the SCR and 26 % for the SEUR. Additionally, the UTES thermal efficiency of approximately 60 % and 52 % were obtained for Cases 1 and 2, respectively.
- Finally, the parametric analysis for case 1 shows that the system performance is affected by changes in the size of the UTES, solar PV size, P2C duration, and P2H duration. When the UTES size increases, its thermal efficiency increases, with P2HC efficiency and energy savings also increasing slightly. Also, when the solar PVT size increases, UTES thermal efficiency and P2HC efficiency decrease. However, the reverse is the case for energy savings, which increase slightly. Finally, the increase in the postponement or shortening of the P2C and P2H duration increases the P2HC and UTES thermal efficiency, with energy savings remaining approximately constant.

A future study will explore the application of this configuration and its control methods for evaluating and comparing the performance of a ground-source water-load (GSWL) heat pump with and without P2HC operation. In addition, a detailed building model of the public school building using Type56 from the TRNSYS component library would be suggested for evaluation of the study in a more realistic simulation environment.

CRediT authorship contribution statement

Fabian Eze: Writing – original draft, Visualization, Validation, Software, Investigation, Formal analysis, Data curation. **Wang-je Lee:** Resources, Investigation, Data curation. **Young sub An:** Resources, Investigation. **Hongjin Joo:** Resources, Investigation. **Kyoung-ho Lee:** Writing – review & editing, Supervision, Methodology, Conceptualization. **Julius Ogola:** Supervision. **Julius Mwabora:** Supervision.

Declaration of competing interest

The authors declare the following financial interests/personal relationships which may be considered as potential competing interests: [Kyoung-ho Lee reports financial support was provided by Korea Institute of Energy Technology Evaluation Planning. Fabian Eze reports financial support was provided by International Center of Inset Physiology and Ecology. If there are other authors, they declare that they have no known competing financial interests or personal relationships that could have appeared to influence the work reported in this paper].

Data availability

The authors do not have permission to share data.

Acknowledgment

This work was supported by the Korea Institute of Energy Technology Evaluation Planning (KETEP) through the research project "Innovative Energy Remodeling Total Technologies for the Aging Public Buildings (No. 20202020800360)" and the Partnership for Skills in Applied Sciences Engineering and Technology – Regional Scholarship and Innovation Fund (PASET-RSIF) by International Center of Inset Physiology and Ecology (ICIPE).

Appendix A. Supplementary data

Supplementary data to this article can be found online at https://doi.org/10.1016/j.enconman.2024.119013.

References

[1] Ossei-Bremang RN, Eze F, Anane-Fenin K, Kemausuor F. Choice modelling of ecooking adoption by households in ghana. Int J Sustain Eng 2024;17:1–13. https://doi.org/10.1080/19397038.2024.2327832.
[2] IEA. World Energy Outlook 2023. Int Energy Agency 2023:1–355.

[3] IEA. World Energy Outlook 2022. Int Energy Agency 2022.
[4] Sezen K, Gungor A. Comparison of solar assisted heat pump systems for heating residences: A review. Sol Energy 2023;249:424–45. https://doi.org/10.1016/j.solener.2022.11.051.
[5] Liu L, Zhao Y, Chang D, Xie J, Ma Z, Sun Q, et al. Prediction of short-term PV power output and uncertainty analysis. Appl Energy 2018;228:700–11. https://doi.org/10.1016/j.apenergy.2018.06.112.
[6] Kim P, Cho S-B, Yim M-S. Examination of excess electricity generation patterns in south korea under the renewable initiative for 2030. Nucl Eng Technol 2022;54:2883–97. https://doi.org/10.1016/j.net.2022.03.021.
[7] Dasí-Crespo D, Roldán-Blay C, Escrivá-Escrivá G, Roldán-Porta C. Evaluation of the spanish regulation on self-consumption photovoltaic installations. A case study based on a rural municipality in spain. Renew Energy 2023;204:788–802. https://doi.org/10.1016/j.renene.2023.01.055.
[8] Maestre VM, Ortiz A, Ortiz I. Sustainable and self-sufficient social home through a combined PV-hydrogen pilot. Appl Energy 2024;363:123061. https://doi.org/10.1016/j.apenergy.2024.123061.
[9] Eze F, Egbo M, Anuta UJ, Ntiriwaa O-BR, Ogola J, Mwabora J. A review on solar water heating technology: Impacts of parameters and techno-economic studies. Bull Natl Res Cent 2024;48:29. https://doi.org/10.1186/s42269-024-01187-1.
[10] Lienhard N, Mutschler R, Leenders L, Rüdisüli M. Concurrent deficit and surplus situations in the future renewable Swiss and European electricity system. Energy Strategy Rev 2023;46:101036. https://doi.org/10.1016/j.esr.2022.101036.
[11] Ordóñez Mendieta ÁJ, Hernández ES. Analysis of PV self-consumption in educational and office buildings in spain. Sustainability 2021;13:1662.
[12] Roldán-Fernández JM, Burgos-Payán M, Riquelme-Santos JM. Impact of domestic PV systems in the day-ahead Iberian electricity market. Sol Energy 2021;217:15–24.
[13] Denholm P, Arent DJ, Baldwin SF, Bilello DE, Brinkman GL, Cochran JM, et al. The challenges of achieving a 100% renewable electricity system in the United States. Joule 2021;5:1331–52.
[14] Tabassum S, Rahman T, Islam AU, Rahman S, Dipta DR, Roy S, et al. Solar energy in the united states: development, challenges and future prospects. Energies 2021;14:8142.
[15] Yildiz B, Bilbao JI, Roberts M, Heslop S, Dore J, Bruce A, et al. Analysis of electricity consumption and thermal storage of domestic electric water heating systems to utilize excess PV generation. Energy 2021;235:121325. https://doi.org/10.1016/j.energy.2021.121325.
[16] Liao W, Kim C, Xiao Y, Kim H, Hong T, Yin S, et al. Quantifying Photovoltaic surplus at an urban scale: A case study in Seoul. Energy Build 2023;298:113523. https://doi.org/10.1016/j.enbuild.2023.113523.
[17] An Y, Kim J, Joo H-J, Lee W-J, Han G, Kim H, et al. Experimental performance analysis of photovoltaic systems applied to an positive energy community based on building renovation. Renew Energy 2023;219:119369. https://doi.org/10.1016/j.renene.2023.119369.
[18] Shafiullah M, Ahmed SD, Al-Sulaiman FA. Grid integration challenges and solution strategies for solar PV systems: A review. IEEE Access 2022;10:52233–57. https://doi.org/10.1109/ACCESS.2022.3174555.
[19] Jha K, Shaik AG. A comprehensive review of power quality mitigation in the scenario of solar PV integration into utility grid. E-Prime - Adv Electr Eng Electron Energy 2023;3:100103. https://doi.org/10.1016/j.prime.2022.100103.
[20] Li B, Liu Z, Wu Y, Wang P, Liu R, Zhang L. Review on photovoltaic with battery energy storage system for power supply to buildings: Challenges and opportunities. J Energy Storage 2023;61:106763.
[21] Vaziri Rad MA, Kasaeian A, Niu X, Zhang K, Mahian O. Excess electricity problem in off-grid hybrid renewable energy systems: A comprehensive review from challenges to prevalent solutions. Renew Energy 2023;212:538–60. https://doi.org/10.1016/j.renene.2023.05.073.
[22] Qiu R, Zhang H, Wang G, Liang Y, Yan J. Green hydrogen-based energy storage service via power-to-gas technologies integrated with multi-energy microgrid. Appl Energy 2023;350:121716. https://doi.org/10.1016/j.apenergy.2023.121716.
[23] Sukumaran S, Laht J, Volkova A. Overview of solar photovoltaic applications for district heating and cooling. Environ Clim Technol 2023;27:964–79. https://doi.org/10.2478/rtuect-2023-0070.
[24] Wu R, Wang L, Xu H, Wang X, Ni C, Hong Y. Energy Efficiency Optimization of CCHP Microgrid Energy Hub with Multiple Scenario Model. 2022 5th Int. Conf. Mechatron. Robot. Autom. ICMRA, Wuhan, China: IEEE; 2022, p. 172–6. doi: 10.1109/ICMRA56206.2022.10145727.
[25] Wang Z, Luther MB, Horan P, Matthews J, Liu C. On-site solar PV generation and use: Self-consumption and self-sufficiency. Build Simul 2023;16:1835–49. https://doi.org/10.1007/s12273-023-1007-3.
[26] Gravelsins A, Pakere I, Tukulis A, Blumberga D. Solar power in district heating. P2H flexibility concept. Energy 2019;181:1023–35. https://doi.org/10.1016/j.energy.2019.05.224.
[27] Wołoszyn J. Global sensitivity analysis of borehole thermal energy storage efficiency for seventeen material, design and operating parameters. Renew Energy 2020;157:545–59. https://doi.org/10.1016/j.renene.2020.05.047.
[28] Maruf MNI, Morales-España G, Sijm J, Helistö N, Kiviluoma J. Classification, potential role, and modeling of power-to-heat and thermal energy storage in energy systems: A review. Sustain Energy Technol Assess 2022;53:102553. https://doi.org/10.1016/j.seta.2022.102553.
[29] Buker MS, Riffat SB. Solar assisted heat pump systems for low temperature water heating applications: A systematic review. Renew Sustain Energy Rev 2016;55:399–413. https://doi.org/10.1016/j.rser.2015.10.157.
[30] Kim K, Kim J, Nam Y, Lee E, Kang E, Entchev E. Analysis of heat exchange rate for low-depth modular ground heat exchanger through real-scale experiment. Energies 2021;14:1893. https://doi.org/10.3390/en14071893.
[31] Jakubek D, Ocłoń P, Nowak-Ocłoń M, Sułowicz M, Varbanov PS, Klemeš JJ. Mathematical modelling and model validation of the heat losses in district heating networks. Energy 2023;267:126460. https://doi.org/10.1016/j.energy.2022.126460.
[32] Syed MW, Kazmi WW, Hussain A, Shah SFA, Kariim I, Mehdi AM, et al. Lignin Liquefaction: Unraveling the effect of process conditions and sustainable pathways for biofuel production– A comprehensive review. Energy Conversion and Management 2024;313:118615. https://doi.org/10.1016/j.enconman.2024.118615.
[33] Risco-Bravo A, Varela C, Bartels J, Zondervan E. From green hydrogen to electricity: A review on recent advances, challenges, and opportunities on power-to-hydrogen-to-power systems. Renew Sustain Energy Rev 2024;189:113930. https://doi.org/10.1016/j.rser.2023.113930.
[34] Eze F, Lee W, An Y, Joo H, Lee K, Ogola J, et al. Calibrated Models of Shallow Ground Thermal Energy Storage for Heating and Cooling Applications. Proceeding Int. Heat Transf. Conf. 17, Cape Town, South Africa: Begellhouse; 2023, p. 9. doi: 10.1615/IHTC17.430-180.
[35] Yang C, Wang T, Chen H. Theoretical and technological challenges of deep underground energy storage in china. Engineering 2023;25:168–81. https://doi.org/10.1016/j.eng.2022.06.021.
[36] Eze F, Lee W, An YS, Joo H, Lee K, Ogola J, et al. Experimental and simulated evaluation of inverse model for shallow underground thermal storage. Case Stud Therm Eng 2024;59:104535. https://doi.org/10.1016/j.csite.2024.104535.
[37] Ahmed AA, Assadi M, Kalantar A, Sliwa T, Sapińska-Śliwa A. A critical review on the use of shallow geothermal energy systems for heating and cooling purposes. Energies 2022;15:4281. https://doi.org/10.3390/en15124281.
[38] Holstenkamp L, Meisel M, Neidig P, Opel O, Steffahn J, Strodel N, et al. Interdisciplinary review of medium-deep aquifer thermal energy storage in north germany. Energy Procedia 2017;135:327–36. https://doi.org/10.1016/j.egypro.2017.09.524.
[39] Andrade C, Selosse S, Maïzi N. The role of power-to-gas in the integration of variable renewables. Appl Energy 2022;313:118730. https://doi.org/10.1016/j.apenergy.2022.118730.
[40] Fambri G, Mazza A, Guelpa E, Verda V, Badami M. Power-to-heat plants in district heating and electricity distribution systems: A techno-economic analysis. Energy Convers Manag 2023;276:116543. https://doi.org/10.1016/j.enconman.2022.116543.
[41] Thornton JW, Bradley DE, Blair NJ, McDowell TP, Duffy MJ, LaHam ND, et al. HVAC library mathematical reference. TESSLibs 2014;17:06.
[42] Zangheri P, Armani R, Pietrobon M, Lorenzo P. Heating and cooling energy demand and loads for building types in different countries of the EU. ENTRA NZE 2014.
[43] Emmerich SJ, Persily AK, McDowell TP. Impact of infiltration on heating and cooling loads in U.S office buildings. Natl Inst Stand Technol 2005.
[44] Mathur U, Damle R. Impact of air infiltration rate on the thermal transmittance value of building envelope. J Build Eng 2021;40:102302. https://doi.org/10.1016/j.jobe.2021.102302.
[45] Kim S-B, Oh B-C-C, Shin U-C. A case study for energy consumption characteristics of high school facilities in seoul. J Korean Sol Energy Soc 2016;36:61–9. https://doi.org/10.7836/kses.2016.36.6.061.
[46] Air To Water Heat Pump CX50 | Manufacturer: Chiltrix Inc. n.d. https://www.chiltrix.com/CX50-air-to-water-heat-pump/ (accessed August 12, 2024).
[47] Emmi G, Zarrella A, De Carli M. A heat pump coupled with photovoltaic thermal hybrid solar collectors: A case study of a multi-source energy system. Energy Convers Manag 2017;151:386–99. https://doi.org/10.1016/j.enconman.2017.08.077.
[48] Yang LW, Hua N, Pu JH, Xia Y, Zhou WB, Xu RJ, et al. Analysis of operation performance of three indirect expansion solar assisted air source heat pumps for domestic heating. Energy Convers Manag 2022;252:115061. https://doi.org/10.1016/j.enconman.2021.115061.
[49] Pelella F, Zsembinszki G, Viscito L, William Mauro A, Cabeza LF. Thermo-economic optimization of a multi-source (air/sun/ground) residential heat pump with a water/PCM thermal storage. Appl Energy 2023;331:120398. https://doi.org/10.1016/j.apenergy.2022.120398.
[50] Liravi M, Karkon E, Jamot J, Wemhoener C, Dai Y, Georges L. Energy efficiency and borehole sizing for photovoltaic-thermal collectors integrated to ground source heat pump system: A Nordic case study. Energy Convers Manag 2024;313:118590. https://doi.org/10.1016/j.enconman.2024.118590.
[51] Wang X, Li T, Yu Y, Liu X, Liu Y, Wang S, et al. Energy saving and economic analysis of a novel PV/T coupled multi-source heat pump heating system with phase change storage: A case study in cold zone in China. Energy Convers Manag 2024;312:118574. https://doi.org/10.1016/j.enconman.2024.118574.
[52] Liu W, Huang Y, Zhang XJ, Wang T, Fang MX, Jiang L. Heat pump assisted sorption carbon capture with steam condenser heat recovery in a decarbonised coal-fired power plant. Energy Convers Manag 2024;319:118919. https://doi.org/10.1016/j.enconman.2024.118919.
[53] Bartela Ł, Skorek-Osikowska A, Dykas S, Stanek B. Thermodynamic and economic assessment of compressed carbon dioxide energy storage systems using a post-mining underground infrastructure. Energy Convers Manag 2021;241:114297. https://doi.org/10.1016/j.enconman.2021.114297.